



Specialist Committee on Ships in Operation at Sea (SOS)

The Specialist Committee on Ships in Operation at Sea (SOS) Final Report and Recommendations to the 29th ITTC



1. INTRODUCTION

1.1 Membership and Meetings

The members of the Specialist Committee on Ships in Operation at Sea (SOS) of the 29th International Towing Tank Conference are as follows:

- Jinbao Wang (Chairman), MARIC, China
- Florian Kluwe (Secretary), HSVVA, Germany.
- Dominic Hudson, University of Southampton, UK
- Henk van den Boom, MARIN, The Netherlands
- Sebastian Bielicki, CTO, Poland
- Koutaku Yamamoto, Mitsui, Japan
- Kenichi Kume, NMRI, Japan
- Hideo Orihara, JMUC, Japan
- Se-Myun Oh, SHI, South Korea
- Gongzheng Xin, CSSRC, China

Four Committee meetings were held as follows.

- 17~19, Jan, 2018 CTO, Poland. All members except Henk van den Boom from MARIN attended.
- 10-12, Sep, 2018, Mitsui, Japan. All members except Gongzheng Xin from CSSRC attended.
- 8-10, May, 2019, HSVVA, Germany. All members attended.
- 15-17, Jan, 2020, Samsung Ship Model Basin, Daejeon, South Korea. All members attended.

The AC representative to IMO Prof. Gerhard Strasser attended all the four meetings in order to keep close eye on the progress of the speed/power trial procedure, C_A guideline and provide feedback from IMO/MEPC meetings.



Figure 1: SOS committee photo with Prof. Strasser (4th meeting)

1.2 Contact with ITTC committees

The 29th SOS committee has coordinated and exchanged information with the CFD/EFD, Resistance and Propulsion, and Manoeuvring in waves Committees on relevant issues.

1.2.1 Contact CFD/EFD committee

The committee has contacted CFD/EFD committee on the following aspects: Establish guideline for CFD to get wind coefficient. Initiate and conduct benchmark study for evaluation of CFD applicability to determine the wind resistance coefficients. Shallow water correction using CFD calculations at model and full scale. Monitoring the development of CFD methods for added resistance due to waves.

CFD/EFD committee chair Sofia Werner recommended Prof. Takanori Hino, for expertise in CFD calculations, to attend SOS meeting and provided valuable guidance on how to proceed. SOS will refer to new guideline 7.5-03-01-02 Quality Assurance in Ship CFD Application in guideline on CFD based determination of wind resistance coefficients.

1.2.2 Contact other committees

SOS committee has Contacted R&P committee regarding Load Variation Coefficient example. Contact was made to Prof. Hironori Yasukawa from Manoeuvring in waves committee regarding combined current correction method.

Contact Quality Systems Group to obtain instruction on Uncertainty Analysis matters.

1.2.3 Joint meeting with CFD/EFD and R&P committee

Accurate performance prediction from model test is very important for sea trial, especially those ships performed sea trial usually at ballast condition. For this purpose, during AC meeting in France (2019), a joint meeting with CFD/EFD and R&P committee chair was held on a new method to predict delivered power using CFD/EFD combination. The method obtained k from CFD while other data from model test. Relative factors which may influence k have been extensively studied numerically, including grid shape and size, temperature, large speed range, posture, rudder etc. Model tests were carried out intensively according to ITTC procedure in MARIC towing tank. Delivered power prediction using this method agrees well with sea trial results on two typical sister ships-208k bulk carrier and 20k container ship. It shows that the combination of CFD/EFD method is practical and feasible.

After face to face discussion and Email contact, CFD/EFD and R&P committee agree to refer paper (by Jinbao Wang et al), Feasible study on full scale delivered power prediction using CFD/EFD combination method, in their final reports to full conference.

1.3 Contact with AC chairman about IMO issues

The AC representative to IMO Prof. Gerhard Strasser, attended IMO MEPC 71-74 during this term. Major outcome/comments related to fluid dynamic issues are as follows.

- (1) Major outcome/comments from IMO MEPC 71 meeting.

- IMO has received submission from ITTC with overview on all procedures that have changed after the 28th ITTC
- Either Raven method should be improved with sufficient validation, or a new method should be proposed

(2) Major outcome/comments from IMO MEPC 72-73 meeting

- China has submitted a proposal on Evaluation of ISO15016_2015 MEPC 72-INF.15
- Submission by ITTC on sea trial procedure(7.5-04-01-01:2017) proposed to MEPC73 (MEPC 73/5/7) was accepted by the meeting
- IACS 2014 industry guidelines shall be updated to reflect the new ITTC sea trial procedure

(3) Major outcome/comments from IMO MEPC 74 meeting

- Amendments to MARPOL Annex VI adopted
- Discussions on introduction of EEDI phase 3 and early implementation for container ships as they are far below the current baseline. Without data, the reduction rate cannot be adjusted for container vessels
- Intense discussion on alternative fuels and main focus on new fuels, marine plastic litter
- Some people raised questions about Raven-method unofficially

1.3.1 Comments from AC

Sea trial procedure (2017 version) was highly appreciated by AC – gained much maturity.

ITTC shall have a representative in ISO committee on 15016 sea trial procedures to coordinate.

All modification to guidelines shall be done in word using tracking mode; track-changes

version shall be submitted together with clean version; modified guideline to be sent to QSG Chairman.

1.4 Terms of Reference (TOR) Assigned by the 28th ITTC

1. Address the following aspects of the analysis of speed/power sea trial results:

(1) Shallow water correction

Formulate, validate and recommend a single method for correcting speed/power sea trial measurements for shallow water effects based on first principles, using full scale and model scale tests and CFD analyses of a suitable range of vessel designs and sizes, water depths and ship speeds.

(This task is considered the highest priority for the specialist committee and shall be commenced immediately. If possible, the procedure 7.5-04-01-01.1 shall be updated to incorporate the new procedure. If this is not possible, the specialist committee shall liaise with the Advisory Council on which action to take).

(2) Wave correction

- a. More extensive validation of the present wave correction methods and expand range of application, introduce other methods where necessary.
- b. Monitoring the development of CFD methods for added resistance due to waves.

(3) Wind correction

- a. Guidance on the location and height of the anemometer and whether a dedicated anemometer is necessary.
- b. Investigate limitations of averaging wind correction method and suggest improvements.

- c. Establish guideline for CFD to get wind coefficient.
- d. Extend wind coefficient database for more ships.
- e. Initiate and conduct benchmark study for evaluation of CFD applicability to determine the wind resistance coefficients.

(4) Current correction

- a. Further validation on the present current correction methods.
- b. To find the possibility of using long track on 2 double runs.

(5) Comprehensive correction

- a. Further validation on Extended-Power-Method
- b. More investigation on existing methods for the speed/power sea trial analysis, including the Combined Correction Method presented by H. Yasukawa (Ship Technology Research, Vol.62, No. 3, 2015, pp.173-185.)

(6) Study and validate model-ship correlation factors at different drafts when possible.

(7) Provide a practical guidance for installation of measuring equipment on a propeller shaft with regard to the shaft material properties (e.g. G modulus), shaft geometry and alignment.

(8) Other

- a. Water temperature and density influence on ship's performance
- b. Noise in the measured data during the ship performance assessment and identify the method for filtering it.

- c. Measurement error and influence on power
2. Update the speed/power sea trial procedures 7.5-04-01-01.1 where appropriate.
3. Update guideline to determine model-ship correlation factors at different draft.
4. Explore 'ship in service' issues, to get feedback to towing tanks with respect to:
 - a. Key performance indicators identifying and establishing performance baseline when appropriate.
 - b. More accurate measurement of environmental data, including wind, waves, current, etc, and comparison with hindcast data when available.
 - c. Speed power related info monitoring, including fuel consumption, shaft torque, speed, draught, trim and rudder angle etc.
 - d. On board recording.
 - e. To find possibilities to analyse ship performance, including speed power relation, decrease of ship speed, etc. on a single run.
 - f. The applicability of unmanned (flying, floating or underwater...) vehicles and devices.
5. Monitor the new information and communication (ICT) technologies applied on board ships to collect and process data as well as ship control systems, and identify their influence on ship performance prediction.

2. SHALLOW WATER CORRECTIONS

2.1 General

Speed power trials are preferably conducted in deep water because the EEDI and contract speed are specified for ideal conditions. Especially for large or fast ships, the actual water depth at the trial's location may be such that a speed loss is incurred. In such cases trial procedures such as ISO 15016:2015 and ITTC 2017, allow for a speed correction according to a formula proposed by Lackenby (1963).

In 2004 at the start of the STA-Joint Industry Project (Boom, Huisman and Mennen 2014), comparisons of trial results conducted by the same ship in both deep- and shallow water clearly indicated that the formula published by Lackenby cannot be considered accurate.

The verification of the Lackenby formula by means of model tests is complicated due to the limited width of model basins which affects the results in shallow water far more than in deep water.

Raven (2012) studied the effects of shallow water on resistance by means of both model testing and potential flow calculations, in order to develop a correction method for the limited width of the model basin. He found that much of the resistance increase in shallow water is actually viscous resistance rather than wave resistance.

Based on these results, Raven (2016) developed a new correction method for shallow water effects in speed power trials. In this so-called "Raven method", the main dimensions and block coefficient determine the viscous resistance of the ship and its increase in shallow water is estimated. The wave resistance is supposed unaffected as long as the depth Froude number is limited; but an additional correction for the effect of the increased dynamic sinkage is applied. This effect on the power increase has

been formulated by Raven based on the Tuck formula for squat (Tuck & Taylor 1970), extended by an estimate for deep water sinkage. The Raven procedure thus estimates the power increase in shallow water at equal speed. This procedure fits in the “Direct Power Method” utilized by both ITTC2017 and ISO15016:2015 to correct the measured power for shallow water effects.

With the continued support of the STA-Group, systematic full scale speed power trials were conducted by MARIN on board three vessels. Two vessels were trialled in 4 water depths and one vessel was trialled in 3 water depths.

The trials were conducted in full compliance with ISO 15016:2015 and ITTC2017 and the measured results were analysed with the free-ware STAIMO (www.staimo.org). The weather conditions during each of these trials were close to ideal; corrections for wind and waves were negligible to small.

For each ship and each water depth, the shallow water effects were computed with both the old method of Lackenby and the new Raven method. The results demonstrated that the Raven method consistently provides more accurate results. These results are presented in the 28th ITTC (2017) Proceedings. Figure 2 to Figure 5 wrap up these results.

Based on this information the 28th ITTC included the Raven method in the Procedure 7.5-04-01-01.1 for speed/power trials next to the existing Lackenby method.

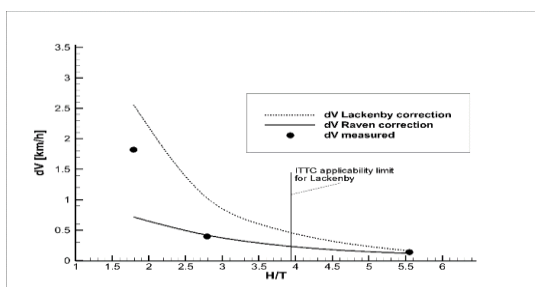


Figure 2 Raven and Lackenby compared to trial results for inland vessel [ITTC 2017]

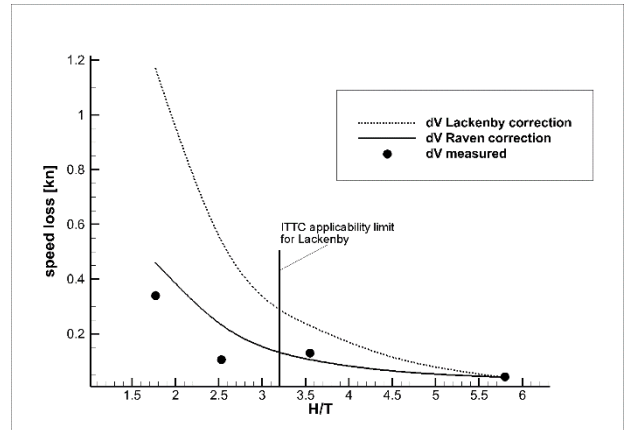


Figure 3 Raven and Lackenby compared to trial results for hopper suction dredger [ITTC2017]

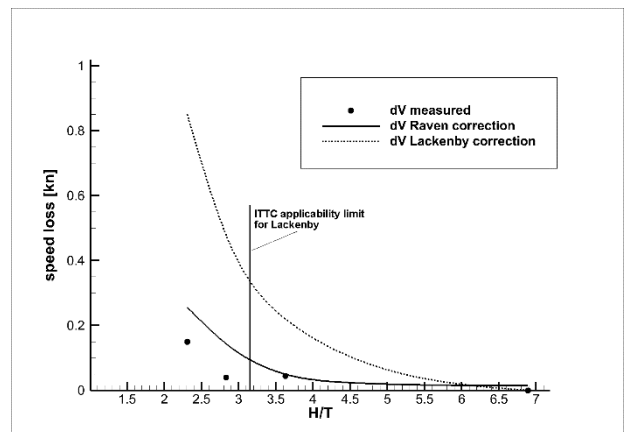


Figure 4 Raven and Lackenby compared to trial results for research vessel [ITTC2017]

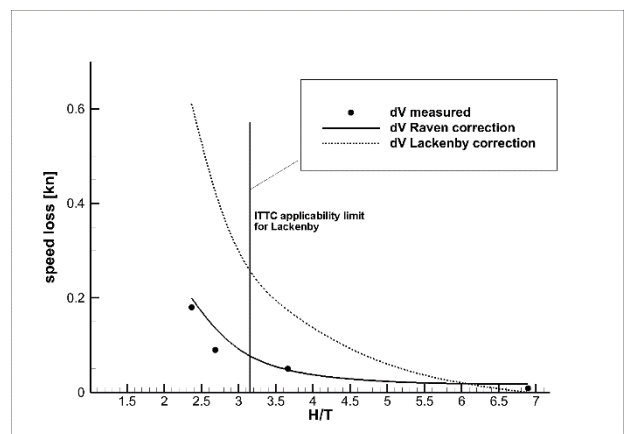


Figure 5 Raven and Lackenby compared to trial results for LPGC on single run [ITTC2017]

2.2 Scope of 29th ITTC SOS

In 2017 the 28th ITTC assigned the new SOS Committee with the following tasks:

Further validation of Raven (2016) method and comparison with Lackenby

More investigation of model tests on shallow water correction

To study the possibility of CFD method on shallow water correction

The three vessels deployed by MARIN and STA-Group for the speed power trials to validate the Raven method, comprised an inland tanker, a hopper suction dredger and a research vessel. These vessels comprised a series of different hull geometries and the trials covered a solid range of water depths.

Although scaling of measurement results to larger sizes is still considered reliable by the ITTC community, the Conference desired a more extensive validation with full scale trials with representative large merchant vessels to be conducted by multiple members.

The 29th ITTC SOS Committee noted that the trial results of the fourth vessel, presented to the 28th ITTC, a 80,000 m³ LPG carrier trialled on two water depths by HHI, should be rejected. Although the results were reasonably in line with those of the other three vessels, the trials on the 80 k LPGC did not comply with ITTC2017 procedure as they were conducted with single runs and therefore the effect of current was not eliminated in the presented results. Therefore, these results have to be neglected.

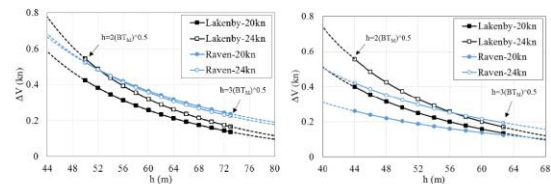
To further validate the Raven method and compare it with Lackenby, the 29th ITTC SOS Committee aimed for an additional extensive and dedicated speed power trial campaign on various large merchant vessels such as ultra large container vessels, very large bulkers and LNG carriers in both deep and shallow water.

At the same time it was envisaged that these trials would be accompanied by systematic model tests on both deep and shallow water and by in-depth CFD analysis. In this way a better understanding of the shallow water effects on speed power was anticipated and a solid shallow water correction method for speed power trials would be achieved. This work was to be shared by the key members of the ITTC SOS Committee.

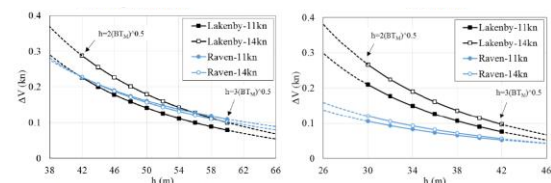
2.3 Evaluation

Several Chinese institutes lead by SSSRI evaluated ISO 15016:2015 and the ITTC 2017 Procedures for speed power trial analysis. Comparisons between the Raven and Lackenby methods were made by applying them to the results of existing speed power trials. In most cases the corrections provided by Raven were found to be smaller than those from Lackenby.

It was concluded by the participating institutes that the Raven method has a solid scientific background and has been validated by the dedicated speed power trials on different water depths (MEPC72/INF.15, 2018).



Correction of speed through shallow water of a Container at EEDI(Left) and light load(right) condition



Correction of speed through shallow water of a Bulk carrier at EEDI(Left) and light load(right) condition

Figure 6 Evaluation of Raven method (MEPC72/INF 15, 2018)

2.4 Model Tests & Physics

The extensive numerical and experimental work of Raven (2012, 2016, 2019) on shallow-water effects in resistance and propulsion over the last decade has been closely reviewed by the SOS Committee. The published results provided a good basis for the understanding of the physics involved. It also presented the concerns and limitations of model testing for shallow water conditions. The width of most basins used for shallow water testing is too small for reliable results and test results thus require a sophisticated correction and extrapolation method.

The large difference of the measured model resistance in deep and shallow water was presented and explained by Dr Hoyte Raven to the ITTC SOS Committee in their Hamburg meeting in May 2019. The Committee solutions for the long-standing problem of the power and speed of ships in shallow water including the correction method for speed power trials.

In 2011 Raven introduced a first step to correct for the effect of the limited width of model basins. At that time no method was available to correct for this, i.e. to translate the model resistance in the tank to that in a waterway of unlimited width and equal depth. By analyzing the flow field from several computations, the nature of the tank wall effect was established, and a new theoretical method developed. It requires a single potential flow computation; evaluation of some fluxes from the result, and solution of an algebraic equation to obtain corrected model speeds. Thus, the measured resistance points are shifted to a slightly higher speed by an amount that depends on water depth, speed and hull form. It then appears that the limited tank width exaggerates the apparent water depth dependence. After the correction, the true water depth effect appears to be a lot smaller.

But there is another important aspect. Model tests are ‘extrapolated’ to full scale to derive a ship performance prediction. The straightforward application of common model-to-ship

extrapolation methods would include the shallow water resistance increase entirely in the ‘wave’ or ‘residual’ resistance component, which is assumed equal for model and ship. Much of the resistance increase in shallow water is actually viscous resistance.

Computational studies (Raven 2019) have indicated that this viscous resistance increase is in most cases a similar percentage for model and ship, and should be included in an increase of the form factor. This is the method now applied at MARIN. It reduces the assumed water-depth dependency of the ship resistance. Both steps have substantially improved the power predictions for ships in shallow water.

Starting with the deep water resistance curve, the two dominant empirical contributions from the shallow water correction method were added: the increase of the viscous resistance, and the increase of resistance due to the additional dynamic sinkage. In Figure 7 this process is visualized and results for the actual ship model are presented.

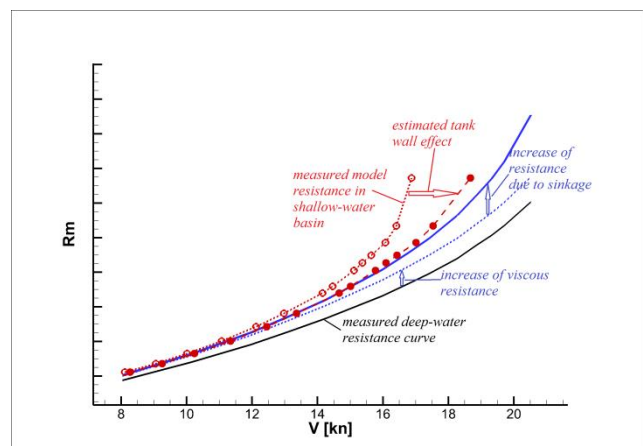


Figure 7 Model test results in deep water corrected to shallow water and compared with model tests results in shallow water [Raven]

A good correlation was obtained with results of the model tests in MARIN’s Shallow Water Basin (220 x 16 x 1.0 m), corrected for the tank wall effect.

The remaining discrepancy was the shallow water increase of the wave resistance, which, contrary to previous insights, turns out to be small.

2.5 Full Scale Trials

Although serious plans were developed in China to contribute with dedicated speed power trials with large merchant vessels on different water depths, these plans did not materialize over the past three years due to lack of confidence, costs and time constraints.

Dedicated systematic trials on large merchant vessels happen to be more complicated and cumbersome than anticipated.

Effectively over the term of the ITTC SOS Committee, no new results of shallow and deep water trials have been delivered or collected.

2.6 CFD Analysis

As part of the agreed validation effort, CTO conducted a correlation study comparing the Raven correction method with CFD results.

The CFD analysis were conducted with the RANS-code STARCCM for the KRISO-containership in 6 water depths ranging from real shallow to deep water. The numerical flow analyses were conducted with double body and free surface effects. The computational domain is presented in the adjacent Figure 8.

For each of the water depths, the resistance was computed and also calculated with the Raven method in combination with the available deep water model test results.

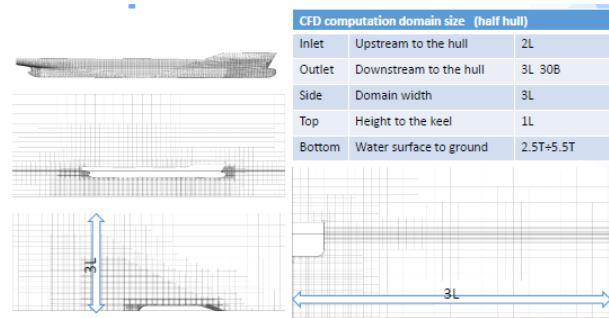


Figure 8 Domain used for KCS in shallow water

The correlation is summarized in the graph below. It is noted that some water depths are outside the application limits of the Raven method. These cases are therefore excluded from the validation conclusion.

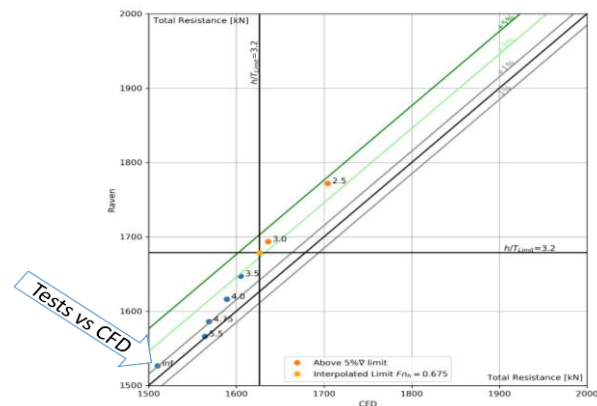


Figure 9 Correlation between Raven (vertical axis) and CFD (horizontal axis) for KCS.

It was concluded by CTO that the difference of the Raven correction compared to the CFD resistance does not exceed 3% below cases with $Fr_h = 0.675$. It was also noted that the estimated sinkage has a significant result on the results.

This implicates that if a better practical empirical sinkage prediction method would be available, the results of Raven could even be improved further.

Although this correlation study included only one vessel design, this important contribution by CTO supported the correlation data obtained from the full scale trials as well as the correlation work conducted by Raven based on model tests and full scale data.

It was also concluded by ITTC SOS that RANS CFD can be used for computing the effects of shallow water on the resistance and propulsion and offers a powerful tool for extrapolating model test results in physically restricted model test facilities.

At the same time, it is noted that RANS CFD unfortunately does not offer a practical correction method for shallow water effects experienced during speed power trials as the geometry of the vessel on trial is normally not disclosed by designers and yards.

2.7 Water Depth Limits

In the current Procedure there is an upper limit for water depth. This limit has no rational background and causes discontinuity in the speed trial results after correction for water depth.

For the Raven method the minimum water depth limits have been investigated: The corrections may be applied for water depths compliant with: $h \geq 2.5 T$ and $h \geq 2.4 V^2/g$

Furthermore, the displacement change due to dynamic sinkage is limited to 5%.

2.8 Propeller Efficiency

An increased resistance normally leads to an increased propeller loading, resulting in a decrease of the propulsive efficiency. For the resistance increase due to wind and waves, this is evaluated using results of overload tests.

Some members noted that it would be consistent to do the same for a shallow water resistance increase. However, as discussed by Raven (2012), the situation is a bit different. In shallow water, not only the resistance increases, but also the wake fraction increases markedly. On the one hand the propeller loading increases more quickly than just due to the resistance increase, normally causing a drop of the open-

water efficiency η_0 ; on the other hand also the hull efficiency

$$\eta_H = (1-t)/(1-w) \quad (1)$$

increases, which partly compensates the drop of the open-water efficiency. Therefore, only counting the drop of the open-water efficiency may not be an improvement.

Based on several model tested cases evaluated, it was concluded that the propulsive efficiency η_D should be considered unaffected by water depth, so no use should be made of the propeller load variation tests for shallow water effects.

2.9 Conclusion

Based on the available validation results from dedicated full scale trials, model tests and RANS CFD analysis, and appreciating the physically rational background of the method, ITTC SOS Committee concluded that the Raven method adopted by ITTC2017, together with the new application limits for water depth, speed and sinkage, provides a consistently more accurate correction for the effect of shallow water on the speed power performance of ships compared with the method presented by Lackenby in 1965.

Therefore, the Lackenby method shall be considered outdated and obsolete and is therefore removed in ITTC 2021 Procedure 7.5-04-01-01.2021.

ITTC shall actively propose to ISO to revise ISO15016:2015 accordingly and to implement the Raven method as the single method for correction of the effects of water depth in analysis of measured speed-trial results.

3. WAVE CORRECTION

3.1 Introduction

There are several empirical methods to correct wave-added resistance at full scale in the sea trial procedure of ITTC (2017) version. However, the STA methods are limited to head waves. For wave encounter angles beyond 45 degrees, the NMRI method can be used, but the method needs the ship's lines. For this reason, an open and transparent semi-empirical SNNM method has been developed. It considers the full range of wave directions and can be applied when a lines plan is not available.

The SNNM method originated in the framework of EU funded FP7-SHOPERA project (2013-2016) (Papanikolaou et al., 2015) at the National Technical University of Athens, which has carried out long research on nonlinear sea-keeping and added resistance (see, e.g., Papanikolaou & Nowacki, 1980; Papanikolaou & Zaraphonitis, 1987 & 1993; Liu et al., 2011; Liu & Papanikolaou, 2016). The method was extended at the Nanyang Technological University (Liu & Papanikolaou, 2020) and verified by the Marine Design and Research Institute of China (MARICAR, 2016-2018; Liu et al., 2019).

An early version of the ensuing formula was submitted to IMO for consideration by member states in support of the research undertaken in SHOPERA (MEPC 70/INF.30, 2016). The formula has been undergoing continuous update with the growing data sample of the established experimental database, as documented in various publications (Liu et al., 2015; Liu et al., 2016; Liu & Papanikolaou, 2016a & 2019 & 2020).

The formula considers the main ship dimensions, global hull form characteristics and speed, along with the ensuing wave conditions, which are directly related to the wave-induced added resistance. This leads eventually to an approximation of the transfer function of the added resistance R_{AW} in regular waves of amplitude ζ_A

and of any direction (head to following), which can be used in power correction during sea trial.

A database of experimental data for the added resistance of about 130 ships of all types has been established to support the development of this formula. The database, which has been continuously enriched over the last 10 years, includes at the moment about 1,500 data points for head wave conditions and another 1,500 data points for other headings, thus, in total slightly more than 3,000 experimental data points. The majority of this data refers to public domain model experimental data and the rest to confidential data from funded research and Joint Industry Projects of the developers.

Figure 10 shows the breakdown of the ships in the database per ship type, which fairly represents the breakdown of the world fleet.

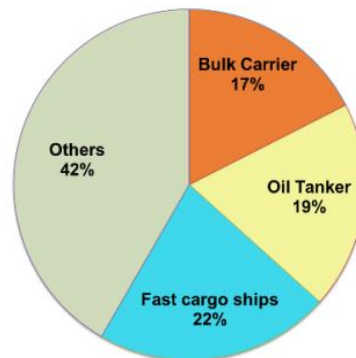


Figure 10 Breakdown of ship types in the database

Figure 11 shows several main particulars and coefficients of the ships in the database. The majority of the ships in the SNNM database are within the range of: $75 \text{ m} < L_{PP} < 383 \text{ m}$; $5.0 < L/B < 7.5$; $2.0 < B/T < 8.0$; $0.54 < C_b < 0.87$. The Froude number covers the typical range of ships in sea trial, i.e., from 0.10 to 0.30. Regarding the associated wave heading, most of the tank tests cases were for head waves (180 degree) only, whereas for bow waves, 21 sets of data were available and for astern waves 11 sets. Attention should be paid in the application of the formula in case the subject ship or type is not within the set limits and the coverage of the database.

The application of the SNNM formula requires 9 input parameters, as listed in Table 1.

Table 1 Example of input file of sample bulkcarrier

| # | Item | Values |
|---|---|--------|
| 1 | Lpp (m) | 280.0 |
| 2 | Beam B (m) | 45.0 |
| 3 | Draft at F.P. Tfore(m) | 16.5 |
| 4 | Draft at A.P. Taft (m) | 16.5 |
| 5 | Block coefficient Cb | 0.86 |
| 6 | kyy; radius of gyration of pitch, % Lpp | 0.25 |
| 7 | Length of waterline entrance(m) | 42.0 |
| 8 | Length of waterline run(m) | 60.9 |
| 9 | Froude number | 0.13 |

Main features of the ships, and the tested Froude numbers and the wave headings in the added resistance database are illustrated in following figures.

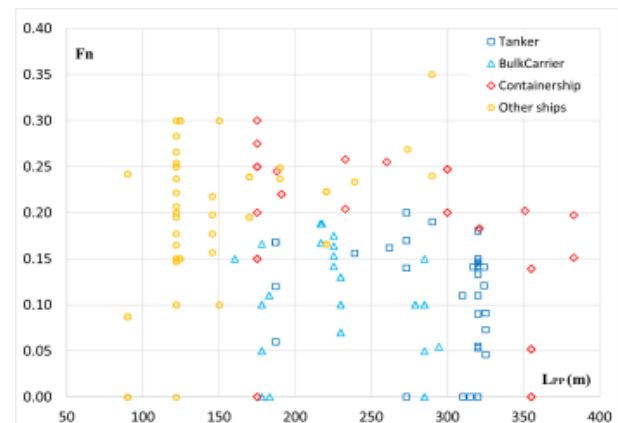
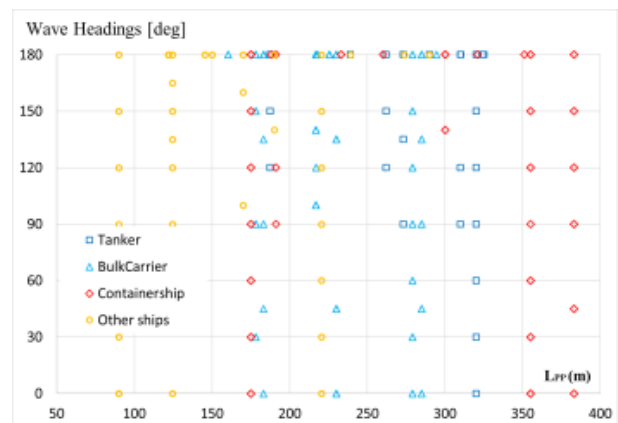
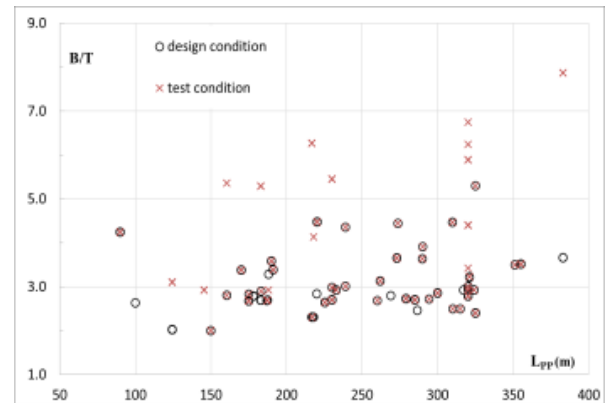
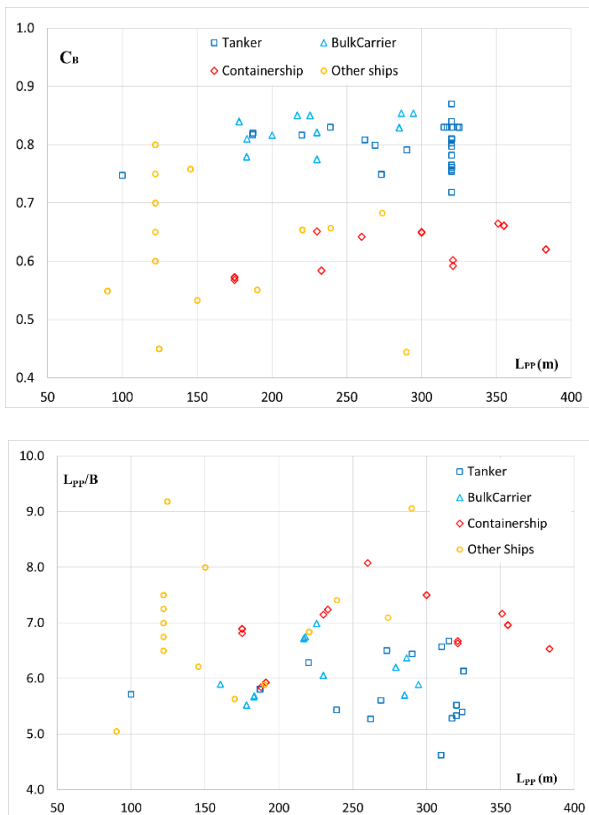


Figure 11 Main features of the ships, and the tested Froude numbers and the wave headings in the added resistance database.

3.2 Self-Validation Study

Figure 12 (top) shows the obtained results of the SNNM formula for the added resistance of the S-cb84 ship at $F_n=0.12$ in comparison with experimental results (Yasukawa et al., 2019). Figure 12 (bottom) shows the obtained results for the added resistance of a large

container ship in ballast condition $F_n=0.197$ in comparison with experimental results obtained at MARIN, Netherlands. An overall good agreement has been observed for two cases.

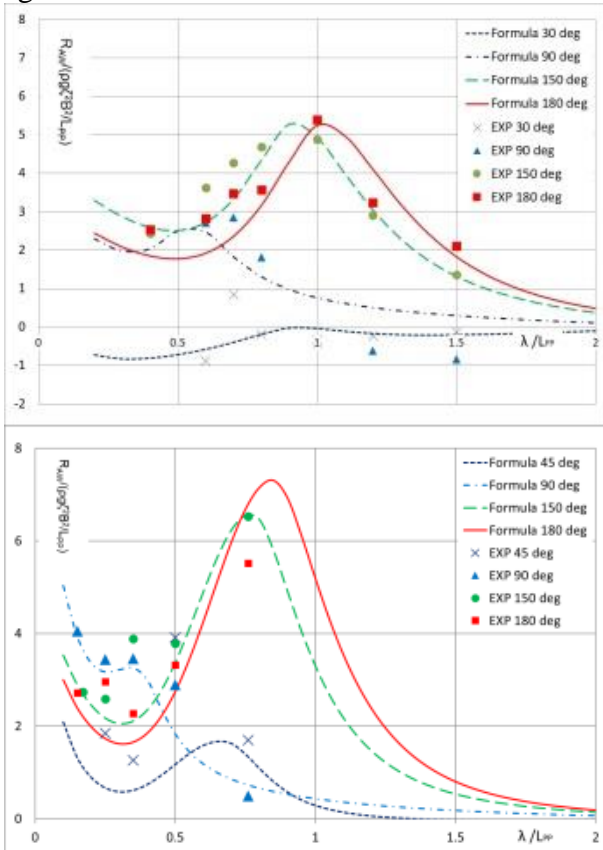


Figure 12 Added resistance of the Scb84 (top) and a large containership (bottom) in regular waves.

Some typical results of the SNNM method in comparison to other methods recommended by ITTC are shown Figure 13.

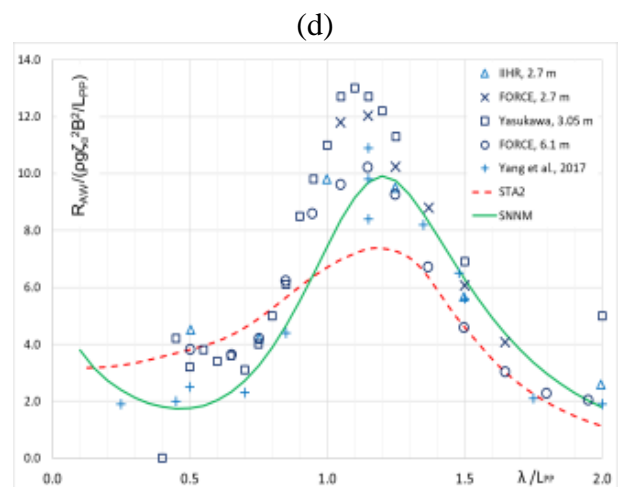
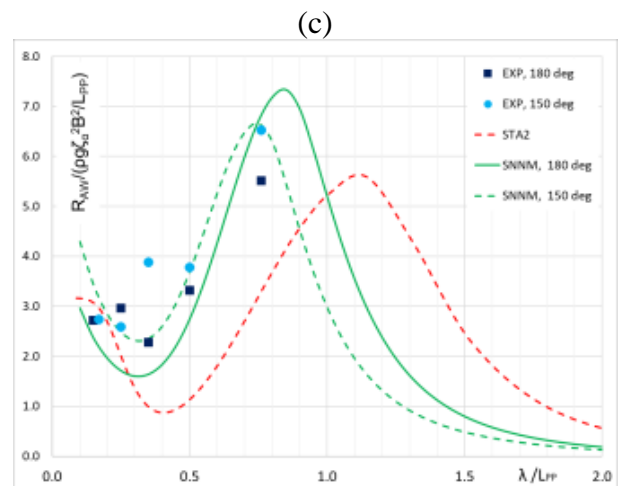
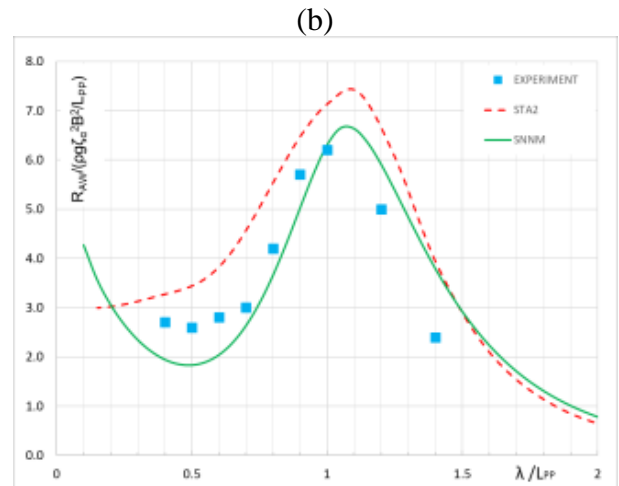
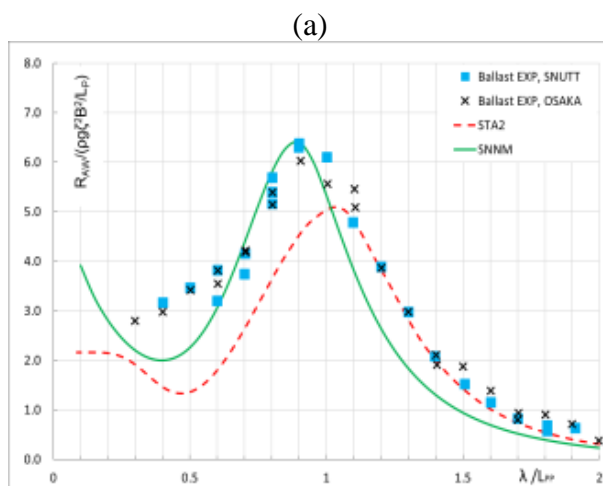
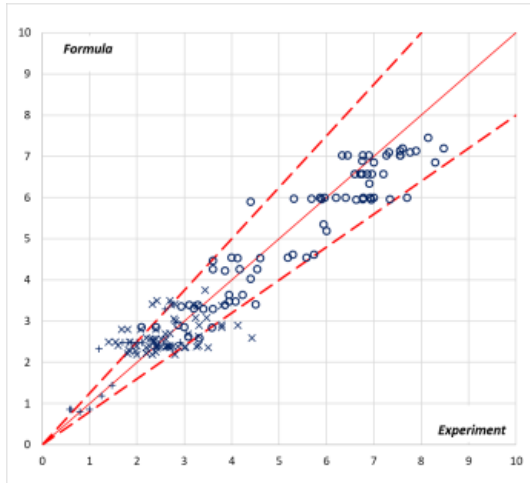


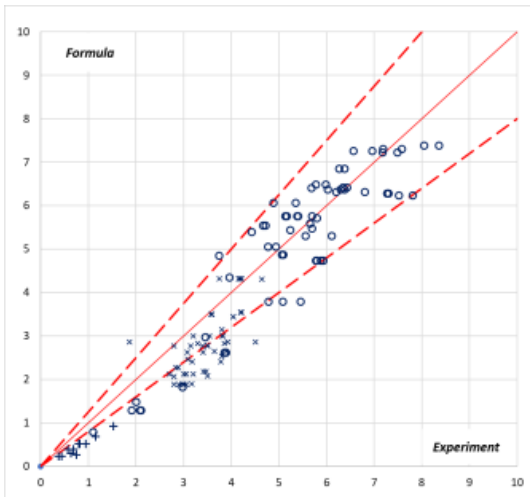
Figure 13 Added resistance of several ships in regular waves: (a) KVLCC2 in ballast condition, $F_n=0.142$; (b) a LNG carrier, $F_n=0.20$; (c) a containership in ballast condition, $F_n=0.197$; (d) KCS in design condition, $F_n=0.26$.

A more systematic validation study is presented in Figure 14 below.

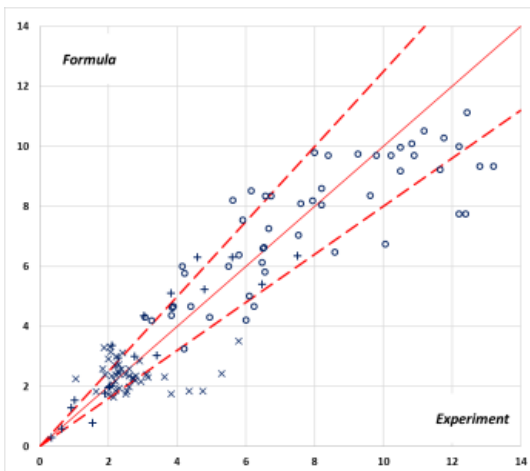
(a)



(b)



(c)



(d)

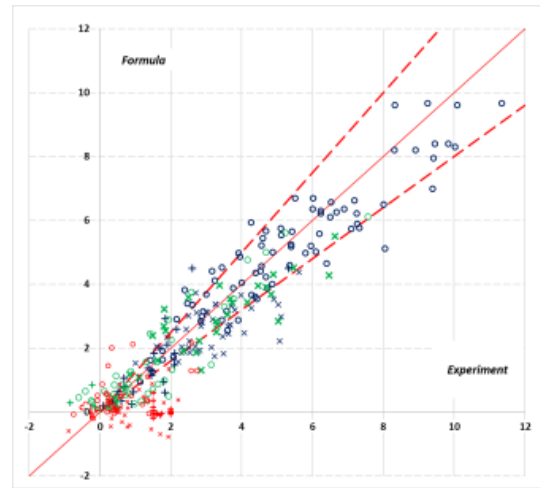


Figure 14 Predicted versus experimental non-dimensional added resistance of ships of different categories in regular waves. (x: $\lambda/L \leq 0.7$; o: $0.7 < \lambda/L < 1.5$; +: $\lambda/L \geq 1.5$).

Figure 14 (a) presents the correlation of the predicted added resistance of eight (8) full type ships (tankers and bulkers) in design load condition in regular head waves at design speed with the experimental results, with the mean percentage error being $\epsilon_{\text{mean}} = -1.3\%$; the Pearson's R correlation coefficient $R = 0.956$; the standard deviation $\sigma = 0.624$; and the Mean Absolute Error $\text{MAE} = 0.499$. Note that σ and MAE are calculated in terms of the non-dimensional added resistance

$$\sigma = R_{AW} / (\rho g \zeta_A^2 \frac{B^2}{L_{PP}}) \quad (2)$$

Figure 14 (b) presents the correlation of the predicted added resistance of six (6) full type ships in ballast condition in regular head waves at design speed in comparison with experimental results, with the obtained $\epsilon_{\text{mean}} = -21.9\%$; $R = 0.948$; $\sigma = 0.777$; $\text{MAE} = 0.657$. Note that the majority of the herein used experimental data is from tested models of small length, namely 2.9 m, thus some uncertainty may be inherent in the experimental data.

Figure 14 (c) is the correlation of the predicted added resistance of seven (7) fast cargo

ships in design load or ballast condition in regular head waves at moderate speeds ($F_n=0.183-0.3$) with the experimental results., with the obtained $\epsilon_{\text{mean}} = 1.6\%$; $R = 0.918$; $\sigma = 1.37$; $MAE = 0.999$.

Figure 14 (d) shows the predicted added resistance of six ships (6) of lengths 175 m ~ 383 m in design load or ballast conditions in regular waves of random headings at moderate speeds ($F_n=0.183-0.3$) in comparison with experimental results. The comparison in bow waves with $120^\circ < \alpha \leq 180^\circ$ is presented in blue with obtained $\epsilon_{\text{mean}} = -4.8\%$; $R = 0.939$; $\sigma = 0.846$; $MAE = 0.640$. The comparison in beam waves with $60^\circ < \alpha \leq 120^\circ$ is presented in green with obtained $\epsilon_{\text{mean}} = 6.4\%$; $R = 0.869$; $\sigma = 1.017$; $MAE = 0.703$. The comparison in stern waves with $0^\circ \leq \alpha \leq 60^\circ$ is presented in red with $\epsilon_{\text{mean}} = -10.2\%$; $R = 0.462$; $\sigma = 0.742$; $MAE = 0.542$. Note that the measurements of the added resistance in astern waves are prone to large uncertainties, hence, the obtained rather low correlation R. However, the achieved $\sigma = 0.614$ and $MAE = 0.459$ are even smaller than that in other headings.

3.3 Preliminary Validation by Some Members of ITTC SOS Committee

Dr. Orihara from JMUC presented the validation results of a 160k DWT crude oil carrier at the 4th Meeting of the SOS Specialist Committee held at Daejeon. Figure 15 shows the results in head to beam waves. Note that here

$$K_{AW} = R_{AW} / \left(4\rho g \zeta_A^2 \frac{B^2}{L_{PP}} \right) \quad (3)$$

Overall, predictions based on the SNNM formula are slightly lower than the experimental results. This is a satisfactory outcome, considering that in prediction a 15% error in added resistance is generally acceptable, as the added resistance is a derived seakeeping quantity of higher numerical and experimental uncertainties are expected. For more accurate predictions,

high-fidelity methods (frequency and time-domain 3D panel codes, CFD or model testing) can be employed.

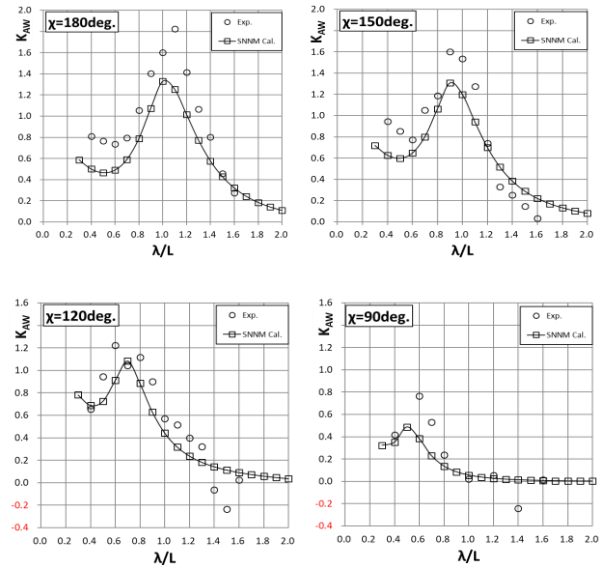


Figure 15 Added resistance of a 160k DWT crude oil carrier in regular waves of various directions, $F_n=0.13$.

MARIN also conducted a correlation study (Grin 2014, Grin & Boom, 2020), comparing the SNNM method with MARIN's STA- & SPAWAVE methods and the 3D panel code FATIMA, using 2 ROPAX, 1 cruise ship and 2 VLCCs (including the well-known KVLCC2).

Figure 16 shows the prediction of the added resistance for MARIN's VLCC in 2 loading conditions in head waves. For the design condition, SPAWAVE considerably under-predicts the peak value. STA2 and SNNM yield comparable peak values but the location of the peak value from STAWAVE2 shifts towards shorter wave region. On VLCC, the SNNM results show an asymptotic increase towards short waves, while the other two methods assume a constant tail value. In ballast condition, similar performance has been observed in the very short waves region. All three methods capture well the transition of the added resistance from short wave to the peak value. However, available tank tests stop at about $\lambda/L_{pp} \approx 0.8$, hence, the peak value and its location cannot be identified by this experiment.

Similar phenomenon is also observed for the KVLCC2 case and the results based on SNNM method agree with model test results quite well.

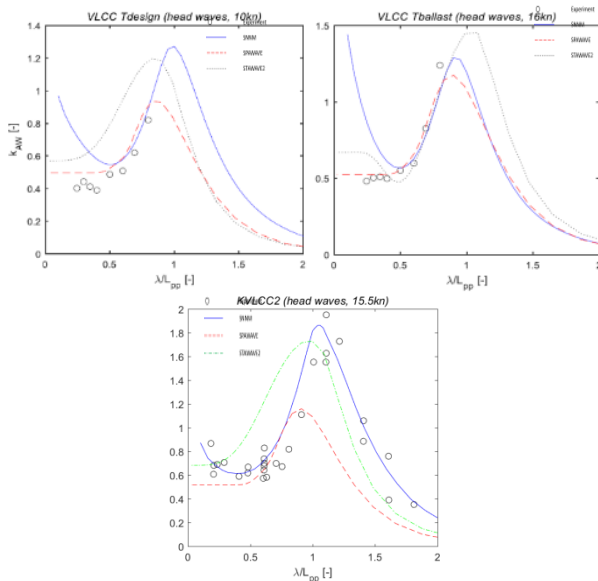


Figure 16 Added resistance of a VLCC at design and ballast conditions and KVLCC2 at design condition in regular head waves.

Two RoPaxs were studied by MARIN and Figure 17 shows the case where the results of added resistance in waves of various headings are available. In head waves, the performance of three methods in short waves is similar to that of the VLCC case. They capture well the added resistance in the transition region, with small deviations in capturing the peak value and its location. In the long waves region, SNNM underpredicts the added resistance and the other two methods have better performance. In bow quartering waves, SNNM underpredicts the added resistance in the long waves region. SPAWAVE captures herein well the experimental results; the result of STAWAVE2 is herein not included. In stern oblique waves, SNNM captures well the experimental results, while SPAWAVE results are a bit lower. There is no experimental data available in the long waves region.

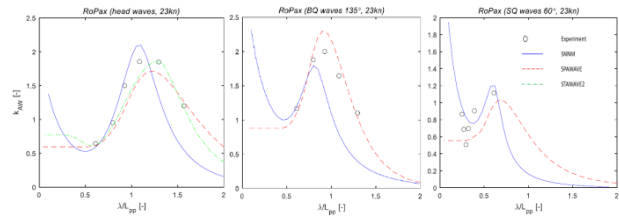


Figure 17 Added resistance of a RoPAX ship in regular waves of various directions, $Fn=0.30$.

Dr. Bielicki from CTO, Poland supplied the validation results of KCS container ship model in following waves of $\lambda/L_{pp}=0.4\sim 1.8$ at two speeds corresponding to $Fn=0.13$ and 0.22 . As presented in Figure 18, at $Fn=0.13$ the added resistance is rather small and the SNNM method, besides showing the same tendency as model test, slightly underpredicts the added resistance in longer waves. At $Fn=0.22$, the SNNM method predicts the added resistance with high accuracy except for the point at $\lambda/L_{pp}=0.4$. Overall, the prediction based on SNNM method for this standard model in following waves is very encouraging.

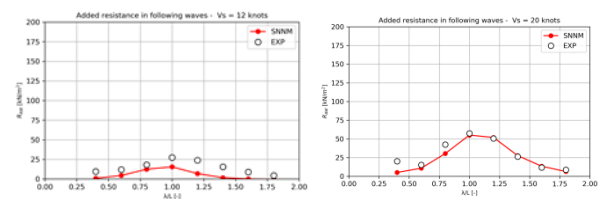


Figure 18 Added resistance of the KCS model in regular following waves, $Fn=0.13$ and 0.22 .

Overall, the validation results from ITTC members demonstrated that the proposed SNNM method well predicts the added resistance of common cargo ship types, particularly bulk carriers, tankers and container ships, which represent the main bulk of the world fleet, in wave of arbitrary directions, and it is fully transparent and readily applicable by engineers in practice. Its performance in predicting the added resistance of passenger ships seems less satisfactory, but may be further improved by enriching the background database. In very short waves, the new SNNM method shows an increasing asymptotic behaviour, which is observed in the experimental results of a large

container ship, a 160K oil tank and the KVLCC2. This is different from other empirical methods.

3.4 Open Validation by ITTC SOS Committee

Encouraged by AC to make more valuable contribution, SOS has carried out more extensive and intensive validation of SNNM method.

After two months' discussion, criterion have been set in $[0, 45^\circ]$ and $(45^\circ, 180^\circ]$ with Pearson's correlation coefficient not less than 0.78 and 0.70 respectively. And relative error between SNNM and experiment over total resistance was also proposed as voluntary index.

Eight SOS members contributed 1477 data points for 29 ships, covering different ship types with different draft, speed and wave direction. Data analysis and report were performed by CTO and HSVA. Pearson's correlation coefficient has reached 0.86 in both wave regions. The relative error distribution has a Gaussian distribution character with average estimated expected value nearly 0% and 75% of samples are within $\pm 2\%$ interval.

After full discussion, SOS agreed to include SNNM method into the sea trial procedure.

4. MONITORING THE DEVELOPMENT OF CFD METHODS FOR ADDED RESISTANCE DUE TO WAVES

As stated in the final report to the 28th ITTC (ITTC 2017), CFD methods have developed to the point where they can be routinely applied to the prediction of wide range of aspects relating to ship hydrodynamic performances.

For the application of CFD methods to the wave correction in the analysis of speed/power sea trials, it is necessary for the methods to be able to predict the added resistance due to waves over a range of wave frequencies sufficient for covering encountered conditions anticipated

during speed/power sea trials and in arbitrary wave headings from head to following directions.

Based on the considerations mentioned above, some examples of recent research works were reviewed to assess the state of the art of CFD application to the prediction of added resistance due to waves.

Kim M. et al. (2017a) presented CFD simulations using a commercial code STAR-CCM+ with an unstructured grid system for KVLCC2 in fully loaded condition under regular head wave conditions. The results were compared with the published model test data (Lee et al. 2013 and Sadat-Hosseini, 2013). It is showed that while the variation of added resistance with incident wave lengths are reasonably reproduced in CFD results, the quantitative agreement in added resistance of CFD results with model tests were not good in particular in short wave lengths where differences are in the order of 20%. (see Figure 19).

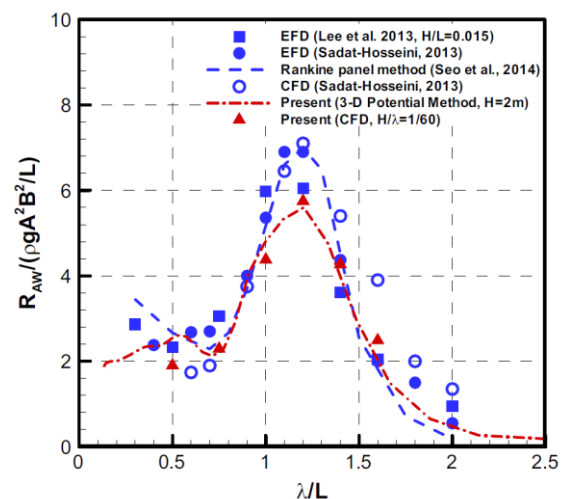


Figure 19 Added resistance ($V_s = 15.5$ knots, $\theta = 180^\circ$). (Kim M. et al. 2017, KVLCC2 in head waves)

Kim Y.-C. et al. (2017) presented CFD simulations using a code WAVIS with a structured grid system for KVLCC2 in fully loaded condition under regular head wave conditions. The results were compared with their model tests results and the published model test data (Sadat-

Hosseini, 2013). It is showed that while the variation of added resistance with incident wave lengths are reasonably reproduced in CFD results, the quantitative agreement in added resistance of CFD results with model tests were not good in particular in short wave lengths where differences are in the order of 10~20%. (see Figure 20).

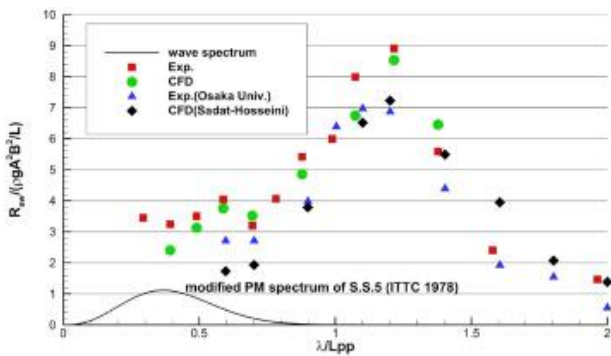


Figure 20 Added resistance in waves. (Kim Y.-C. et al. 2017, KVLCC2 in head waves)

Hossain M.A. et al. (2018) presented CFD simulations using a code CFDSHIP-IOWA with an overset structured grid system for KRISO container ship in fully loaded condition under regular head wave conditions. The results were compared with their model tests results and the published model test data (Simonsen 2013, Sadat-Hosseini, 2015). It is showed that while the variation of added resistance with incident wave lengths are reasonably reproduced in CFD results in the same way as the previous KVLCC2 cases, the quantitative agreement in added resistance of CFD results with model tests were not good in particular in short wave lengths where differences are in the order of 40%. (see Figure 21). Also noted is that the differences among model tests data were quite large corresponding to the order of 50% in short waves.

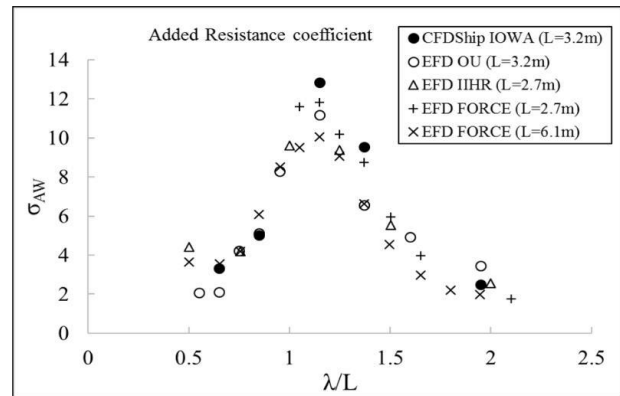


Figure 21 Added resistance coefficient. (Hossain M. A. et al. 2018, KCS in head waves)

Ohashi K. et al. (2019) presented CFD simulations using a code CFDSHIP-IOWA with an overset structured grid system for KRISO container ship in fully loaded condition under regular head wave conditions. The results were compared with their model test results. It is showed that while the CFD results agree reasonably well with model tests results in longer waves ($\lambda/L > 1.0$), the quantitative agreement in added resistance of CFD results with model tests were not good in short wave lengths where differences are in the order of 20%. (see Figure 22).

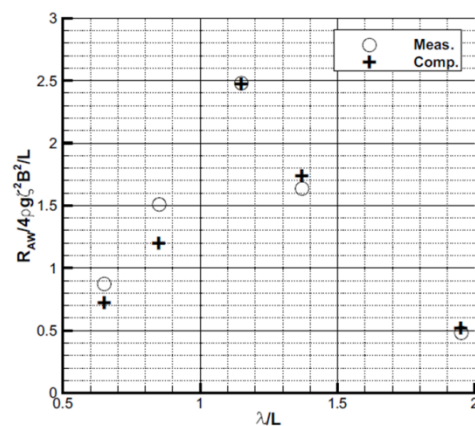


Figure 22 Comparison of an added resistance coefficient. (Ohashi et al. 2019, KCS in head waves)

Guo and Wan (2019) presented CFD simulations using a code naoe-FOAM-SJTU with an unstructured grid system for KRISO container ship in fully loaded condition under regular head wave conditions. The results were compared

with the published model test data (Simonsen 2013, Sadat-Hosseini, 2015). It is showed that while the CFD results agree reasonably well with model tests results in longer waves ($\lambda/L > 1.0$), the quantitative agreement in added resistance of CFD results with model tests were not good in short wave lengths where differences are in the order of 20% at the shortest wave case ($\lambda/L = 0.65$). (see Figure 23).

Kim M. et al. (2017b) presented CFD simulations using a commercial code STAR-CCM+ with an unstructured grid system for S175 container ship in fully loaded condition under regular head wave conditions. The results were compared with the published model test data (Fujii and Takahashi 1975, Nakamura and Naito 1977).

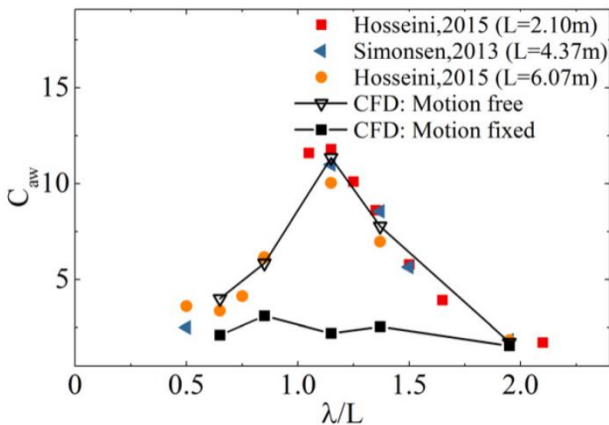


Figure 23 Added resistance coefficient of KCS. (Guo and Wan 2019, in head waves)

It is showed that while the variation of added resistance with incident wave lengths are reasonably reproduced in CFD results, the quantitative agreement in added resistance of CFD results with model tests were not good in particular in shorter waves where differences are in the order of 50% at the shortest wave case ($\lambda/L = 0.7$). (see Figure 24).

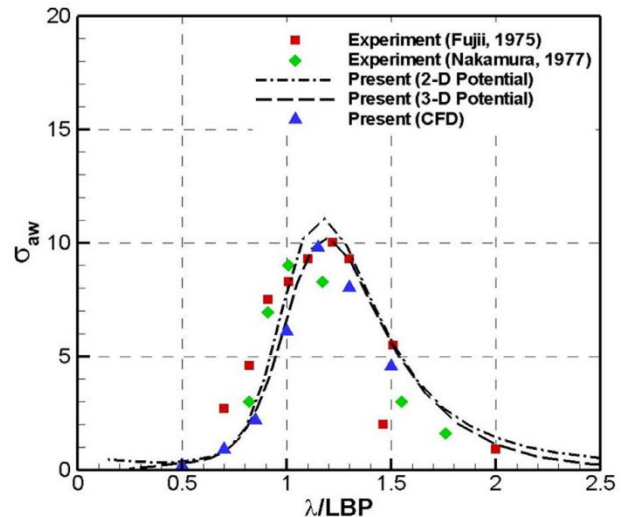


Figure 24 Added resistance comparison ($F_n = 0.25$, $\theta = 0^\circ$). (Kim M. et al. 2017b, S175 in head waves)

Orihara and Yoshida (2018) presented CFD simulations using a code WISDAM-X with an overset structured grid system for a non-public tanker form (called SR221C) in ballast condition under regular head wave conditions. The results were compared with their model test results. It is showed that while the CFD results reproduce the trends of model test results, the quantitative agreement in added resistance of CFD results with model tests were not good in short wave lengths where differences are in the order of 20%. (see Figure 25).

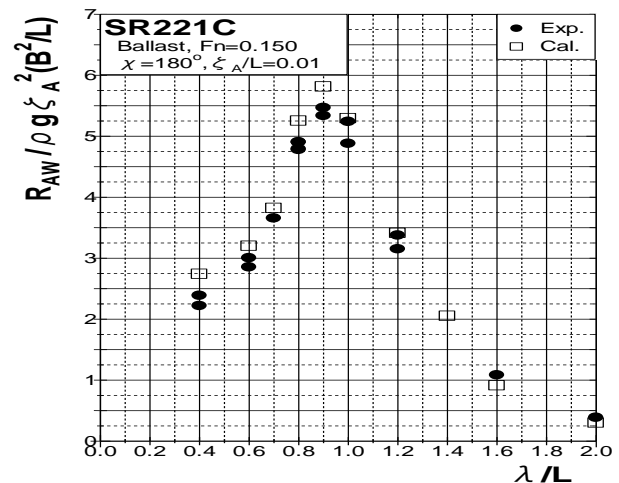


Figure 25 Comparison of normalized added resistance for a SR221C model in ballast condition, $F_n = 0.15$, $\zeta_A/L = 0.01$. (Orihara and Yoshida 2018, in head waves)

As described in the above reviews, most of the CFD studies are conducted only for the case of head waves and fully loaded condition for a limited number of open-source hull forms (e.g., KVLCC2, KRISO container ship). This may be mainly due to the unavailability of suitable model test data for the validation of CFD methods. For wave conditions other than head waves, available tank test data suitable for the validation in speed/power sea trial applications, that is, those at forward speeds corresponding to the speed range of speed/power sea trials are limited to the data of Fujii and Takahashi (1975) for S175 container ship and Sadat-Hosseini et al. (2015) for KRISO container ship. Since these data are for the relatively old hull forms and container ships, validation data for other ship types (e.g. tankers, bulk carriers) are needed for the general examination of the CFD applicability to wave correction in speed/power sea trials. Another issue in the validation of CFD method is that most of them are made for fully loaded conditions and not for the actual trial conditions, although speed/power sea trials are conducted only in trial (lightly loaded) conditions, except for the case of tankers. Model test data for the actual trial conditions and validation with these data are considered indispensable for the rigorous assessment of the applicability of CFD methods to wave correction in speed/power trials analysis. In addition, the accuracy of the model test results must be examined in detail before the validation of CFD methods. As seen in the model test data shown in Figure 19 through Figure 25, variation of model test data for the specific hull forms among different testing facilities are quite large and greater than the difference between the CFD and model test results. Establishment of high-fidelity model test data with small bias and random errors is strongly desired.

It is thus considered that according to the results of present monitoring the development of CFD methods for added resistance due to waves, CFD methods have not matured to the point where they can be generally applicable to the speed/power sea trial analysis for the purpose of correction of wave effects mainly due to the lack

of validation under wave conditions other than head waves and trial (lightly loaded) displacement conditions. It should also be emphasized that CFD methods must be validated against high-fidelity model test data obtained from multiple model testing facilities in order to remove the uncertainty due to inter-facility bias in the model test data.

5. WIND CORRECTION - GUIDANCE ON THE LOCATION AND HEIGHT OF THE ANEMOMETER

Given the importance of estimating accurately the wind effect for correction of measured power from a sea trial, as accurate a determination of the encountered wind speed as possible is essential.

Ideally the undisturbed wind speed encountered by the vessel should be measured, if at all possible. This may be accomplished by deployment of a dedicated measurement buoy equipped to measure wind speed. The results of measuring wind at a buoy and the effects on the speed performance analysed from trials is shown in section 6 (table 3) and seems to indicate that differences are reduced when buoy data are utilised. Technology is developing to allow direct measurement from the ship of the undisturbed wind speed outside the region where airflow is distorted by the presence of the ship. One example of such technology is the use of LIDAR (light detection and ranging), which is used routinely in the offshore wind industry and being tested for use in ship sea trials by MARIN, as described further in section 23. It is therefore strongly encouraged to adopt techniques that measure undisturbed airflow wherever possible for the correction of sea trials.

It is recommended that investigations are conducted to compare such remote measurement techniques with wind speed and direction as measured onboard in order to better recommend the instrumentation necessary for making wind measurements during trials.

Comparison of wind speeds predicted using weather hindcast models with those measured by standard ship anemometers indicate that onboard measurements are considerably in excess of those from a hindcast model, even accounting for the difference in vertical location of the anemometer and the reference height of model predictions (Lakshmyanarayana and Hudson, 2018). Adopting a standard power-law in correcting for vertical location is a further source of uncertainty when comparing measurements from buoys, other vessels and weather models.

If an anemometer is to be used for trials measurements then it should be positioned so as to minimise the effect of airflow distortion on the measured wind speed. Siting on a foremast away from superstructures is preferable, although it should be appreciated that even at the foremast the airflow is still disturbed by the presence of the ship. Within certain bounds agreement is found between wind speed measured by a foremast anemometer and as measured by an anemometer at the superstructure, as shown in section 6.

Computational fluid dynamics (CFD), or wind tunnel experiments, may be used to assist with anemometer positioning. Any error in measurement is highly dependent on the anemometer position and the shape of the ship's superstructure. Shipboard anemometers on typical tankers/bulk carriers may not be well-exposed and the wind could be accelerated by over 10% or decelerated by 100% (Moat et al, 2005a). There have been studies using wind tunnels and CFD aimed at improving measurement of wind speed on research vessels and on providing guidance for the correction of wind speed measured by merchant ships participating in the Voluntary Observing Ship (VOS) programme of the World Meteorological Organisation (WHO) (Moat et al, 2005a,b, 2006 a,b).

Moat et al (2006 b) provide non-dimensionalised predicted wind speed bias data that may

be used directly to guide placement of anemometers onboard vessels.

In general, the anemometer should be sited as close to the upwind leading edge of superstructures and as high above them as possible. Directly above the leading edge is not recommended due to greater distortion effects at oblique wind angles. Sonic anemometers are to be used in preference to cup anemometers due to the reduced effect of oblique flow angles on reliable measurements. Any anemometer should be sited more than 3x mast diameter away from masts.

6. LIMITATIONS OF AVERAGING WIND CORRECTION METHOD

6.1 General

Estimation of the wind effect is important for the powering performance analysis of the ships. During speed trials, it is common that the wind speed and directions change significantly. Therefore, accurate and reliable on-board measurement of the wind speed and direction is essential for the evaluation of the wind resistance.

The characteristics of wind speed and direction have been investigated for LNG carriers, tankers and large container were performed as shown in Table 2. The ultrasonic anemometers in addition to the shipborne anemometer were installed on radar mast and foremast. Based on these measurements and the influence of the measurement locations and the characteristics of relative wind direction depending on ship headings are investigated.

Table 2 Overview of Measurement Duration and Installation Position

| | 160K LNGC | 180K LNGC | 115K Tanker 1 st | 115K Tanker 2 nd | 20000TEU Container |
|---|---------------|---------------|-----------------------------|-----------------------------|--------------------|
| Duration | 2017.05.01~05 | 2017.06.08~13 | 2017.06.23~26 | 2017.08.22~24 | 2017.05.20~22 |
| Loading Condition | Ballast | Ballast | Full Load | Ballast | Ballast |
| Measure Position (Foremast-FM, Radar-mast-RM) | FM | FM | FM | FM | FM |
| | RM | RM | RM | RM | RM |

Figure 26 and Figure 27 are comparison of wind measurement results. The distributions of the unfiltered wind measurement have large scatter throughout the range (Figure 26).

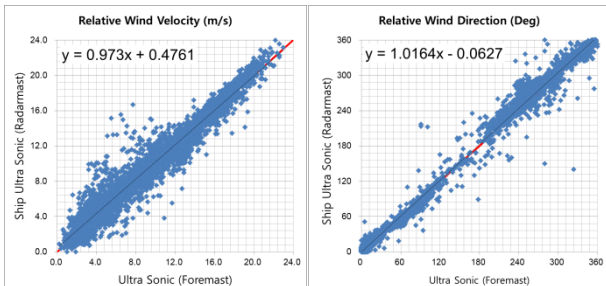


Figure 26 Comparison of Wind Measurement Results: Ultrasonic Foremast VS Shipborne Anemometer

The agreements between wind data from foremast and radar mast are improved by the filtering, confirming that this is an important step in the elimination of the disturbance by super structure. To avoid the influence of structures, measured data are filtered, and limit values for filtering are as follows:

- Rate of Turn < 5 deg / min
- Ship Speed > 5.0knots

As a result of the wind observations, the influence of the position of the anemometer is not significant when the ship's speed is over 5 knots

and rate of turn is less than 5 degrees as shown in Figure 27.

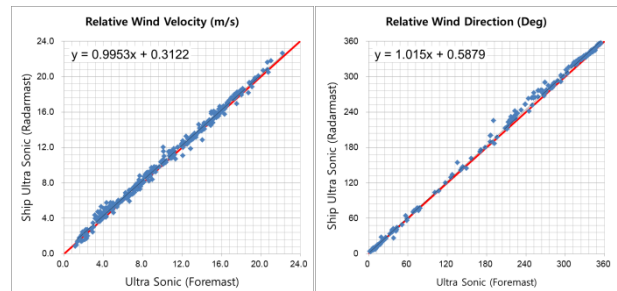


Figure 27 Comparison of Wind Measurement Results after Filtering: Ultrasonic Foremast vs Ship Anemometer

In order to investigate the influence on speed performance analysis by wind averaging process, wind observations from GEOJE weather buoy moored near sea trial area in Korea, and data from on-board measurements were compared. As shown in Table 3, approximately 10% of wind data from GEOJE buoy shows that the speed difference between measurement and calculated by averaging process is over 1 m/s. And more than 30% of wind data from on-board shows over 1 m/s speed difference. For the wind direction, more than 10% of wind data indicate that the difference between measurement and calculated by averaging process is over 40 degrees both from buoy and from ship. The maximum difference of wind direction is about 180 degrees from GEOJE buoy. It means that head wind becomes follow wind.

Table 3 Difference of Wind by Averaging Process for 180K LNGC

| | Speed Difference (m/s) | | | | Direction Difference (degree) | | |
|-----------------------|------------------------|---------|---------|------|-------------------------------|--------|------|
| | > ± 0.5 | > ± 1.0 | > ± 2.0 | Max. | > ± 20 | > ± 40 | Max. |
| GEOJE Buoy | 31% | 10% | 4% | 3.4 | 7% | 4% | 179 |
| Shipborne Radar mast | 78% | 56% | 19% | 6.6 | 20% | 9% | 139 |
| Ultrasonic Radar mast | 60% | 39% | 15% | 5.5 | 23% | 12% | 148 |
| Ultrasonic Foremast | 64% | 37% | 13% | 6.2 | 23% | 11% | 138 |

Table 4 shows the influence of the speed power performance by wind data from different anemometer position.

The relative wind speed difference between the positions of anemometer is estimated in range of -0.03knots to +0.06knots for the 4 cases of speed power trials. The effect of the wind averaging process on speed power performance is mostly around -0.04knots.

Table 4 Effect on the Speed - Power Analysis

| Based on ISO15016:2015 | | Differences by Measurement Location (Relative Wind) | | Speed Difference (knots) | |
|------------------------|------------------------|---|----------------|--------------------------|-----------------------|
| | | Direction (Deg) | Velocity (m/s) | Anemometer Location | Averaging Process *** |
| 180 K LN GC | Shipborne | Base | Base | Base | -0.14 |
| | Ultra-sonic Radar Fore | 5.60 | 1.42↓ | 0.01↓ | -0.07 |
| 115 K Tanker 1st | Shipborne | Base | Base | Base | -0.07 |
| | Ultra-sonic Radar Fore | 1.22 | 0.93↓ | 0.02↓ | -0.03 |
| 115 K Tanker 2nd | Shipborne | Base | Base | Base | -0.07 |
| | Ultra-sonic Radar Fore | 0.20 | 0.77↓ | 0.03↓ | -0.04 |
| 20,000 TEU | Shipborne | Base | Base | Base | -0.04 |
| | Ultra-sonic Radar Fore | 8.17 | 0.85↑ | 0.04↑ | -0.04 |

Notes:*** is Wind data by averaging process - wind data by each speed run

6.2 Limitations of Averaging method

(1) When wind speed is close to the design speed, and the angle between ship direction and wind direction is small, then the relative wind speed approaches zero in tailwind, which is not easy to measure accurately. This will influence the averaging accuracy over double run.

(2) When wind speed reaches BF5, ranging from 17-21kn, for those ships such as Oil tank, Bulk carriers, some Gas carriers, 'real' tailwind will occur, in these cases, averaging method tends to underpredict the ship speed.

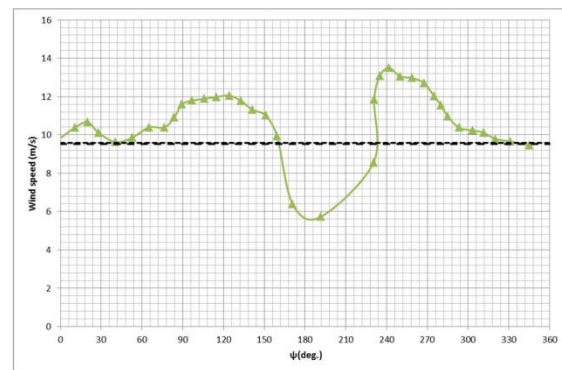


Figure 28 LNG carrier tested in FORCE

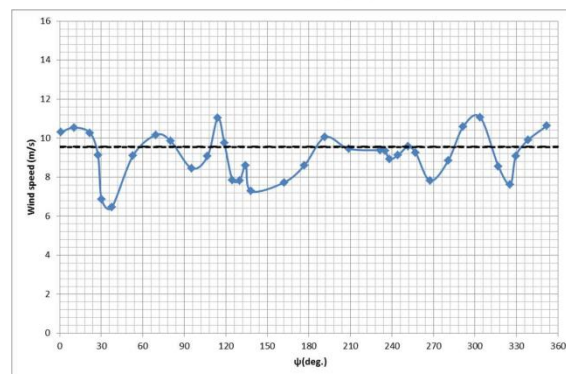
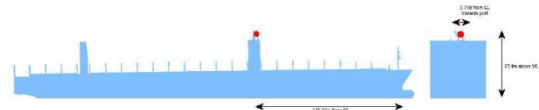


Figure 29 Container ship tested in FORCE

(3) When wind speed reaches BF6, ranging from 22-27kn, for almost all commercial vessels, including container ships, averaging method tends to underpredict the ship speed.

(4) When head wind speed is less than tailwind, averaging method tends to predict higher ship speed than without averaging.

6.3 Conclusions

The Committee decided to retain the present wind correction method. The reason for averaging method is imperfection of on board wind measurements caused by wind disturbances of the vessel i.e the wheelhouse as well as the inaccuracies of instruments such as “cup-type” anemometers. In case the average true wind speed from two subsequent runs is within 5% or 0.5m/s whichever is larger, or the undisturbed (not affected by any part of the ship) wind speed encountered by the vessel is measured remotely by a certified instrument accurately, the averaged single run wind speed may be used.

7. GUIDELINE FOR CFD-BASED DETERMINATION OF WIND RESISTANCE COEFFICIENTS

The guideline for CFD- based determination of wind resistance coefficients was established during the current period of SOS ITTC committee works. The document comprises general practices for computational approach and evaluation methods of CFD based calculations aimed at finding the corrections from wind forces acting on a vessel during sea trials. It is suggested to use as a complementary document to method of Appendix F in 7.5-04-01-01.1.

8. STUDY ON CFD COMPUTATIONS OF WIND FORCES

8.1 Introduction

The influence of wind forces on corrections of Sea Trials measurements plays an important role in the assessment of sea trial ship’s performance. Thus, the committee of the current ITTC term has focused on the applicability of established wind force corrections by use of CFD methods. For this purpose, AC proposed an exercise in which several participants were invited to run CFD computations on two selected cases: a Handy Size Bulk Carrier (HSBC) and a Japan

Bulk Carrier (JBC). Both represent the above water parts of non-existing vessels.

There were four participants working on the HSBC case and seven participants on the JBC case. Both cases were provided by two of the participants and they had differently defined flow conditions. HSBC had free domain size and conditions with uniform velocity on the inlet whilst the JBC focused on the modelling domain in a way to represent wind tunnel conditions. The detailed CFD computation conditions and domain sizes as well as solvers used in the computations are presented in Table 5 and Table 6.

Table 5 HSBC computations parameters

| P#N | TS | NE [106] | TM | BC |
|-----|--------|----------|-----------------|--|
| 1 | 2e-4 | 9.6 | SST | I:V, O:P, N-S on hull, F-S on remaining boundaries |
| 2.1 | | 19.9 | k-ε, realizable | I:V, O:P, N-S on hull, F-S on remaining boundaries |
| 2.2 | | 4.2 | SST k-ε | |
| 3 | Steady | 1.5 | EASM | I:V, O:P, Top, Side – symmetry, remaining N-S |
| 4 | | 9.6 | RSM | |

Table 6 JBC computations parameters

| P#N | TS | NE [106] | TM | BC |
|-----|--------|----------|-----------------|---------------------------------------|
| 1 | Steady | 9.6 | EASM | N-S: bottom, hull |
| 2 | Steady | 8.2 | k-ω, SST 2003 | N-S(W-F): bottom, hull |
| 3.1 | 0.05 | 8.2 | EASM | N-S: bottom |
| 3.2 | 0.01 | 11.3 | k-ε, realizable | |
| 3.3 | | | k-ω, SST | |
| 3.4 | | | RSM QPS | |
| 4.1 | Steady | 27.2 | k-ω, SST | N-S: bottom, hull |
| 4.2 | | 16.9 | | |
| 4.3 | | 11.7 | | |
| 4.4 | | 27.2 | | |
| 5 | 0.0002 | 11.2 | SST | N-S(W-F): hull, F-S: other boundaries |
| 6.1 | Steady | 1.7 | RSM | N-S(W-F): hull, F-S: other boundaries |
| 6.2 | Steady | 4.1 | k-ω, SST | N-S: bottom |
| 7 | Steady | 0.6 | k-ω, SST-Menter | N-S(W-F): bottom, hull |

P#N – participant number, TS – time step, NE – number of elements, TM – turbulence model, BC – boundary condition, I:V-Velocity inlet, O:P-Pressure outlet, F-S - free slip, N-S –no slip wall, W-F – wall function

The participants were numbered in random order and the number behind the dot refers to the calculated cases. Most of the participants elaborated one computational case, however, some provided results for more cases differing in domain details or turbulence models used in the analyses.

8.2 Geometry of Analysed Cases

The geometry of the vessels selected for the computations differ significantly from each other, although the ship type is the same. HSBC (Figure 30) had a smaller number of hatches and a pair of cranes above two of five hatches whilst JBC (Figure 31) was simplified to a version without outfits but with nine hatches on the deck. The superstructure of JBC was modelled by simple blocks and HSBC is characterized by more detailed and realistic geometry. It is worth noting that all participants were free to decide about geometry simplifications for meshing purposes.

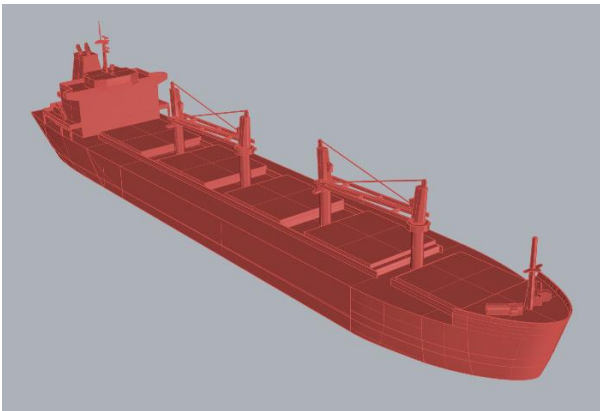


Figure 30 HSBC model

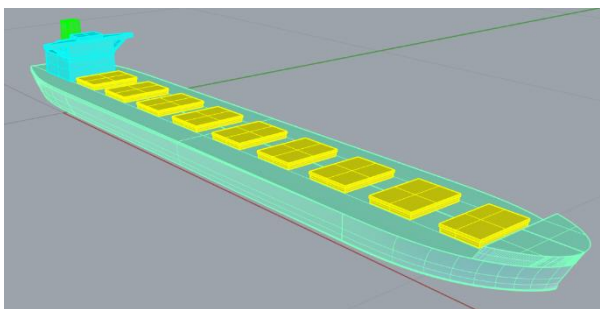


Figure 31 JBC model

8.3 Coordinate System

All calculated results were converted to the unified coordinate system presented in Figure 32. The direction of wind is 0° from aft and 180° for head wind.

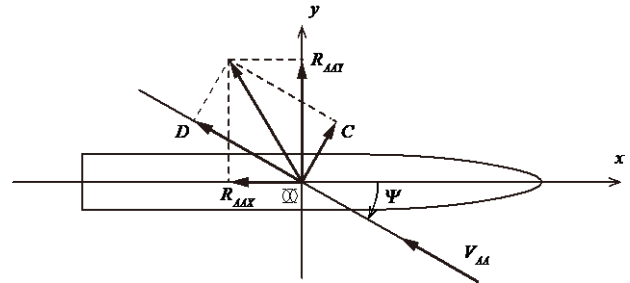


Figure 32 Unified coordinate system

8.4 Post-Processing of Calculated Forces

The most important wind force in Sea Trial analyses is the air resistance acting along the longitudinal axis of the ship, however, the lateral force was also examined. Typically, the wind tunnel results are presented in a normalized form as coefficients – the forces are related to a dynamic pressure multiplied by a reference area. The air force coefficients are computed according to formulas:

$$C_{DAX} = \frac{R_{AAX}}{q_A A_{VX}} \quad (4)$$

$$C_{DAY} = \frac{R_{AAY}}{q_A A_{VY}} \quad (5)$$

where:

C_{DAX}, C_{DAY} – are normalized wind force coefficients

A_{VX} – Transverse projected (frontal windage) area [m²]

A_{VY} – Lateral projected (side windage) area [m²]

$$q_A = \frac{1}{2} \rho_A V_{AA}^2 \quad (6)$$

- dynamic pressure

V_{AA} – reference air velocity, [m/s]
 ρ_A – air density, [kg/m³]

These values of coefficients are presented as a function of the wind velocity direction.

8.5 Calculation Parameters

The study was carried out at model scale corresponding to the model size used in wind tunnel tests (Kaiser, 2016) (Kume, 2019). This approach is necessary to avoid any scale effects. The length of the HSBC model is $L_{PP} = 0.867\text{m}$ and of the JBC is $L_{PP}=1.200\text{m}$. The angles of the wind velocity vectors were set in the ranges from 0° to 30° and 150° to 180° with equal steps of 10° . The inlet velocities were set to 20m/s for HSBC and 25m/s for JBC respectively.

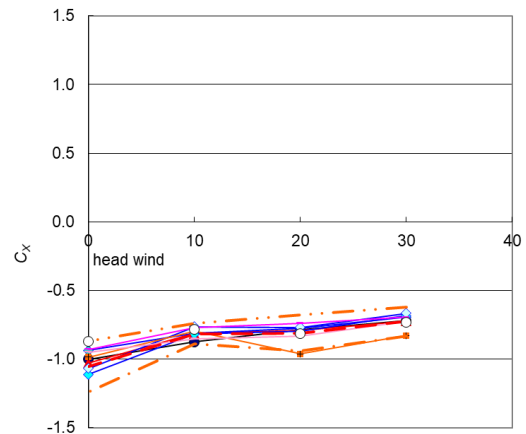
8.6 Averaging Wind Profile

The reference velocity used in normalization of forces measured in the wind tunnel is always captured at a certain level (typically 10 m above sea level at full scale) and may cause some additional discrepancies in comparison between measurements and CFD results. To avoid this effect Kume et al. proposed a method for averaging the wind profile at the centre of the rotation of the model to find the reference speed in a more appropriate way. The details of this method can be found in the new ITTC guideline on the CFD-based Determination of Wind Resistance Coefficients (submitted to this full conference) or Kume (2019, 2020).

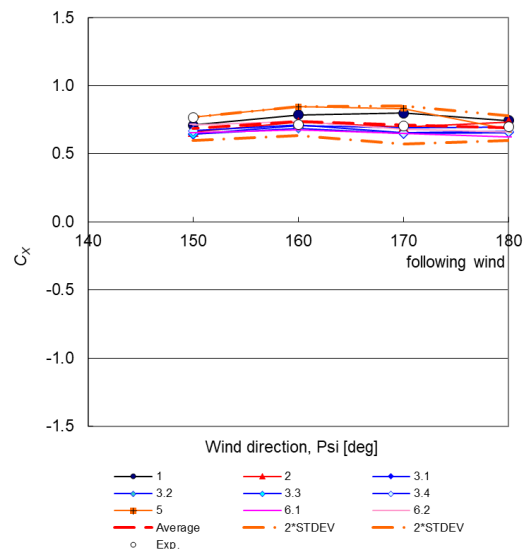
8.7 Forces Coefficients

The CFD results for the HSBC model were obtained using uniform flow, except for one of the participants whilst the majority of the calculations of the JBC case were carried out in a velocity profile caused by the boundary layer. The CFD and wind tunnel longitudinal C_{DAX} and lateral C_{DAY} values of the wind force coefficients plotted over the wind directions showed some scatter of the results in comparison to wind

tunnel results. However, all normalized values are within the doubled standard deviation and the averaged values are close to the experimental curves. The percentage of deviation from the measurements is presented by plotting CFD based normalized values against experiment at the same direction of wind velocity vector.



(a) Headwind side



(b) Following wind side

Figure 33 Comparison of C_x coefficients for JBC

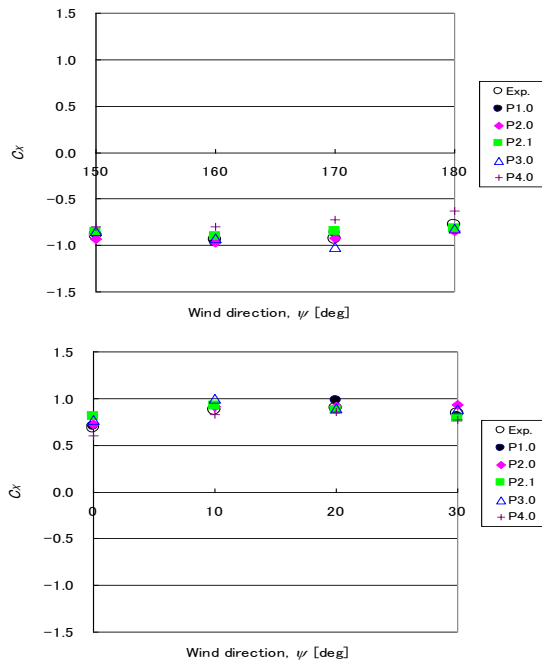


Figure 34 Comparison of C_x coefficients for HSBC

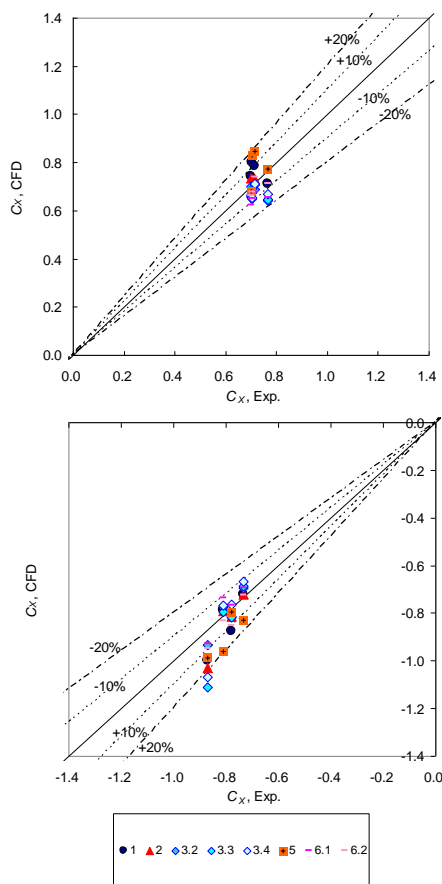


Figure 35 Results of CFD against Wind Tunnel, JBC

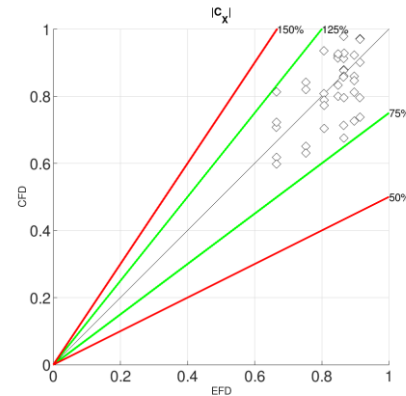


Figure 36 Results of CFD against Wind Tunnel, HSBC

8.8 Discussion of The Results

CFD based normalized wind forces are within $\pm 20\%$ of the experimentally achieved values. This level of deviation means that ITTC allows the use of CFD analyses in the wind correction of a Sea Trials only when the corrected value of the wind force does not exceed 2% of the total corrected power.

8.9 Conclusions

The scattered distribution of results does not lead to a conclusion which methodology of CFD computations is preferable. The main profit of the study is the normalization method of both experimental and calculation forces. This approach allows minimizing the impact of a velocity distribution on the analysed quantities.

8.10 Acknowledgements

The ITTC SOS Committee would like to express heartfelt thanks for all participants of this study followed in alphabetic order of company/institution name: CSSRC (China), CTO (Poland), Lloyd’s Register (Korea), MARIC (China), MARIN (the Netherlands), NMRI (Japan), SJTU (China), SSPA (Sweden), SVA GmbH. (Vienna Model Basin)

9. CURRENT CORRECTION

The current correction in speed trials is conducted by assuming a current variation using the measured ship's speeds.

In general, current speed is considered to change against not only time and but also place. Therefore, in principle, the measurements of speed trial are conducted at almost the same position by repeating double runs, as shown in Figure 37, to eliminate the effect of place.

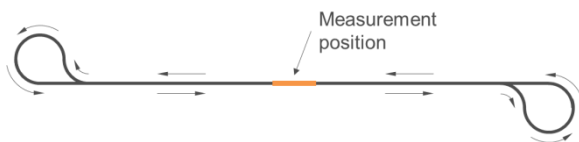


Figure 37 Path for the repetition of double run

The most primitive current correction method is to average the ship's speeds obtained by double run at the same engine output setting (mean method), in which current variation is assumed to be constant during the double run and current speeds are eliminated by averaging ship's speeds of the double run. As the method assuming that the current speed varies against time, mean of means method and iterative method are adopted in the ITTC RP 7.5-04-01-01.1 ver. 2017. The mean of means method assumes that current speed varies parabolically and eliminates the current speeds at each run. On the other hand, in the iterative method, current variation against time is explicitly estimated using all measured ship's speeds and the ship's speeds are corrected by subtracting the estimated current speeds. The Iterative method was newly adopted in the ITTC RP, after validation using a lot of fabricated cases by Strasser et al. (2015). This method has been used in a lot of actual speed trials by a lot of shipyards for three years after being adopted. To date, no implementation problem has been informed to ITTC.

To decrease repetition of double runs, a run procedure called "long track" was proposed. This procedure allows to conduct the conduct of multiple measurements at different points in

each run (between turnings) along the run course, as shown in the Figure 38. The committee discussed this procedure.

If the long track procedure would be adopted, it is required that current variations against time at different measurement positions should be the same as each other to eliminate the effect of place. However, in general, it is difficult to find such area.

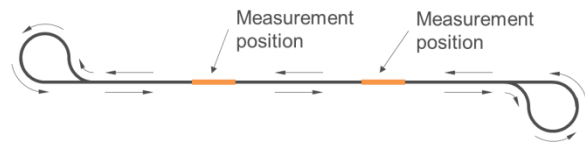


Figure 38 an Example of path for long track

To address this issue, though the concept to make measuring positions close to each other, as shown in Figure 39, was proposed, it was pointed out that such procedure has the following problems.

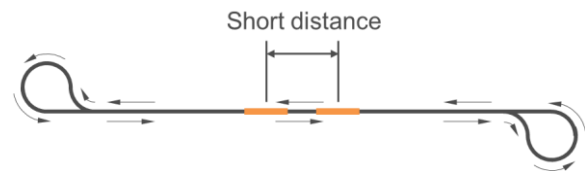


Figure 39 an Example of path for long track

1. As shown in Figure 40, the current variation derived in this procedure might be less reliable than the one derived in normal procedure.

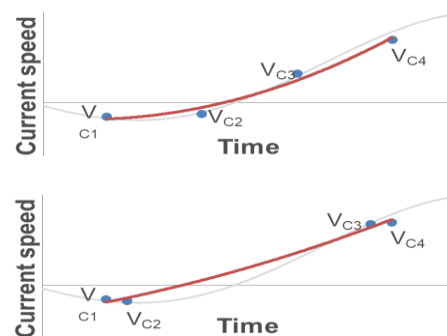


Figure 40 schematic charts describing the difference of current variation between normal procedure (upper) and long track with closed points (lower)

2. Even current speeds at close points might be different from each other. Two current variations derived by analysing the results of actual trial, in which, as shown in Figure 41, two consecutive 1-mile-measurements at almost the same positions in each run were conducted at the same engine output setting for redundancy purpose. The measured data were analysed individually for each position A and B. These results show that the difference of current speeds at two position only 1-mile away was more than 0.1knots.

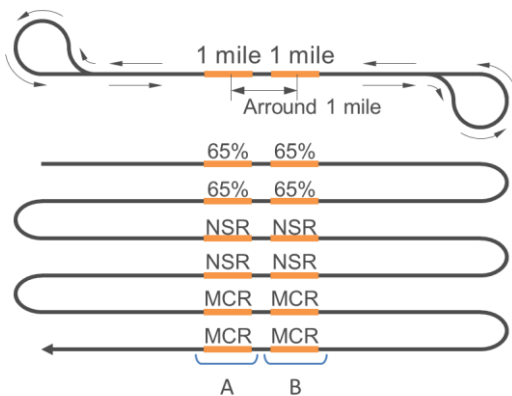


Figure 41 schematic diagram of two consecutive 1-mile-measurements for redundancy purpose

The committee also discussed the order of engine output in long track method. Engine output setting for each measurement should be determined to avoid a deceleration approach, as shown in Figure 43. The data measured after a deceleration approach as shown in Figure 42 might include some uncorrectable gain due to insufficient deceleration, since it is impossible to confirm whether the ship's speed reached the one corresponding to the engine output setting and the sea condition during the measurement.

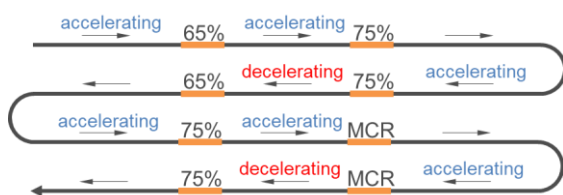


Figure 42 schematic diagram of long track including deceleration approach

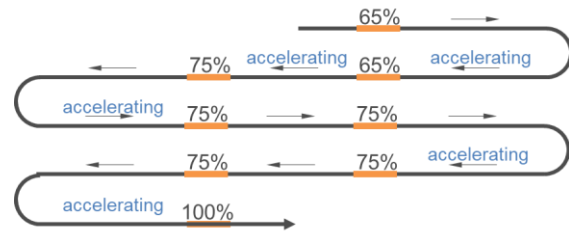


Figure 43 schematic diagram of long track without deceleration approach

The committee concluded that it is premature to adopt the long track procedure at this stage.

10. COMPREHENSIVE CORRECTION

At present, some trial analysis methods are proposed to eliminate the added resistances, such as wind and wave. In this section, the methods directly correcting delivered power by the following equation are reviewed:

$$P_{Did} = P_{Dms} - \Delta P \quad (7)$$

$$\Delta P = \frac{\Delta R V_S}{\eta_{Did}} - P_{Dms} \frac{\Delta \eta}{\eta_{Did}} \quad (8)$$

Where P_{Did} is the delivered power in ideal condition, i.e. the delivered power after added resistances have been eliminated, P_{Dms} is the delivered power in trial condition and ΔP is the added power due to all added resistances. The lower equation is derived considering that the delivered power is derived from ship's speed through the water, V_S , resistance, R , and propulsive efficiency, η_D . In the equation, $\Delta \eta$ is the difference between η_{Did} and η_{Dms} , which are the propulsive efficiencies in ideal and trial conditions respectively.

10.1 DPM

Direct Power Method (DPM) has been already adopted in the ITTC RP 7.5-04-01-01.1. In this method, propulsive efficiency is assumed to vary linearly with the added resistance, as written below:

$$\frac{\Delta\eta}{\eta_{D_{id}}} = \xi_P \frac{\Delta R}{R_{id}} \quad (9)$$

Where ΔR is total added resistance estimated from the measured data and ξ_P is slope of linear function which should be derived from self-propulsion tests (SPT) and load variation tests (LVT) in advance.

From equations (8) and (9), the following quadratic equation for $P_{D_{id}}$ is derived and $P_{D_{id}}$ can be obtained by solving the equation:

$$P_{D_{id}} = P_{D_{ms}} - \frac{\Delta R V_S}{\eta_{D_{id}}} \left(1 - \frac{P_{D_{ms}}}{P_{D_{id}}} \xi_P \right) \quad (10)$$

10.2 EPM

In Appendix J of the ITTC RP 7.5-04-01-01.1, Extended Power Method (EPM) is described as informative. The advantage of this method is to be able to give full scale wake fraction.

In the EPM, propulsive efficiencies for both ideal and trial conditions in equation (9), $\eta_{D_{ms}}$ and $\eta_{D_{id}}$ respectively, are estimated from the propeller open characteristics (POCs) and self-propulsion factors (SPFs) considering both with and without load variation effects.

Especially, propeller efficiencies for ideal and trial conditions, $\eta_{O_{id}}$ and $\eta_{O_{ms}}$, are derived by estimating the propeller loading points for each condition from propeller open chart of the subject vessel, as follows (see also Figure 44).

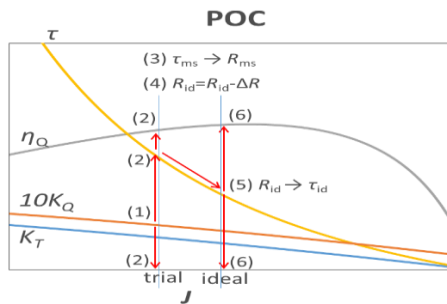


Figure 44 propeller open chart in which how to derive propeller efficiencies as well as propeller advance coefficients, propeller load factors and so on are shown.

The torque coefficient in trial condition, KQ_{ms} , is calculated from the data measured in speed power trial with the following formula:

Propeller advance coefficient, propeller load factor and propeller efficiency in trial condition, J_{ms} , τ_{ms} and $\eta_{O_{ms}}$, corresponding to the above KQ_{ms} are derived from the propeller open chart. (J_{ms} is used to estimate full scale wake fraction)

Ship's resistance in trial condition, R_{ms} , is calculated from the obtained τ_{ms} .

Ship's resistance in ideal condition, R_{id} , is calculated by subtracting the total added resistance due to disturbances, ΔR , from R_{ms} .

Propeller load factor in ideal condition, τ_{id} , is calculated.

Propeller advance coefficient and propeller efficiency in ideal condition, J_{id} and $\eta_{O_{id}}$, corresponding to the above τ_{id} are derived using the propeller open chart.

Full scale wake fraction, w_S , can be estimated in the following process:

Full scale wake fraction in trial condition, $w_{S_{ms}}$, can be derived from the already obtained J_{ms} , n_{ms} and V_S with the following formulae:

$$1 - w_{S_{ms}} = \frac{J_{ms} n_{ms} D}{V_S} \quad (11)$$

The scale correlation factor, e_i , can be estimated from the above $w_{S_{ms}}$ and the $w_{M_{ms}}$ with the following formula:

$$e_i = \frac{1 - w_{S_{ms}}}{1 - w_{M_{ms}}} \quad (12)$$

S_{id} shall be derived from $w_{M_{id}}$ and the above e_i with the following formula:

$$1 - w_{S_{id}} = (1 - w_{M_{id}}) e_i \quad (13)$$

As to validation of the EPM, as already reported in the 28th ITTC proceedings, the differences of the power corrected by between the

DPM and the EPM were less than 1% of that corrected by DPM, as shown in Figure 45.

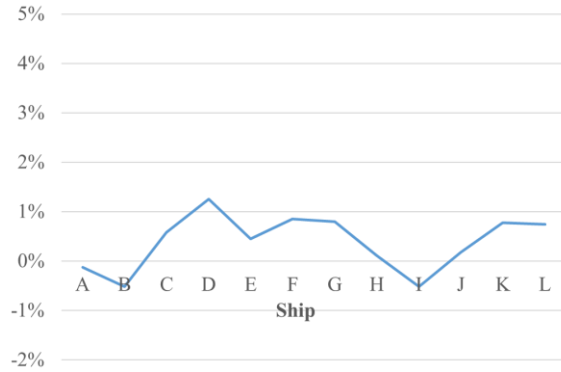


Figure 45 Comparison between the corrected powers by DPM and EPM normalised by the corresponding value by DPM (% DPM)

10.3 Power-based Taylor Expansion Method (PTEM)

Yasukawa (2019) proposed a new method that he calls Power-based Taylor Expansion Method (PTEM).

This method requires ξ_P , and SPFs in both with and without propeller load effects. In this method, P_{Did} (at $n = n_{id}$) as the function of propeller shaft speed is expressed by Taylor series about $n = n_{ms}$, as follows:

$$P_{Did} = P_{Dms} - \Delta n \frac{\partial P}{\partial n} + \Delta n^2 \frac{\partial^2 P}{\partial n^2} + O(\Delta n^3) \quad (14)$$

Where

$$\Delta n = n_{Did} - n_{Dms}. \quad (15)$$

$\partial P / \partial n$ and $\partial^2 P / \partial n^2$ are derived from POCs, SPFs considering the load variation effect and V_s .

The advantage of this method is to require neither added resistances nor current speed to eliminate the influence of disturbances. Total added resistance is estimated by the following function derived by rewriting the equation (10).

$$\Delta R = \frac{\Delta \eta P_{Did}}{\xi_P V_s} \quad (16)$$

V_s is estimated by the following equation:

$$V_s = \frac{P_{Did} \eta_{Did}}{(1 - t_{id}) T_{id}} \quad (17)$$

Where T_{id} is also derived by Taylor series at $n = n_{ms}$.

The above ΔR , V_s , n_{id} and P_{Did} as well as related intermediate information, such as POCs and SPFs and so on, are derived with iterative process.

In order to obtain Δn , the following equation derived by substituting equation (16) and also equation (14) for basic equation (8) is solved:

$$\Delta n^2 \frac{\partial^2 P}{\partial n^2} - \Delta n \frac{\partial P}{\partial n} = \frac{\Delta \eta (1 - \xi_P)}{\Delta \eta + \xi_P \eta_{Did}} P_{Dms} \quad (18)$$

Verification results conducted using virtual trial data are presented. It is concluded that the error of corrected propeller shaft speed and corrected delivered power were less than 1% and 2% respectively within the disturbances taken into account in the verification.

Furthermore, the analysis results by this method using the actual trial data are also presented. It is mentioned that as a result of comparison with other methods, scatter of the results analysed using this method is smaller than that of others.

11. MODEL-SHIP CORRELATION FACTORS AT DIFFERENT DRAFTS

This topic deals with the question whether correlation factors should be determined draft-dependent or not. This has been put on the agenda already several years ago as there has been a certain indication from ships in service that performance on loaded draughts showed a different relation to the prediction as on ballast draught.

The phenomenon is mainly prevalent for ship types where sea trials under normal conditions cannot be performed at design draughts. This in particular affects container vessels. One very sparse example of a container vessel at full load draught is shown in Park, J. et.al. (2016)

Additional relevance is generated by the calculation procedure for the Energy Efficiency Design Index (EEDI) as a statutory instrument for emission control in shipping. Here, the attained EEDI performance is calculated utilizing the predicted relation between speed power performance on ballast draughts and loaded draught.

Gaining evidence in this question has been proven very difficult and in the last couple of years no concluding answers could be found. The reasons are manifold, but primarily the lack of appropriate full scale data of sufficient quality is prohibiting an evaluation.

As statistical evidence is not available to date an alternative approach is to look into physical effects that potentially generate a dependency between the scaling procedure and draught, which subsequently would require draft dependent correlation. The following factors could establish such kind of relationship:

- Varying relation between wave making resistance and viscous resistance components on different draughts.
- Form factor k: In case a ship and draught dependent form factor is applied, the influence of the draught is incorporated in the draught dependent k, while this is not the case for those cases where no specific form factor is used for the prediction.
- Influences from submerged transoms
- Flow separation – varying behaviour on different draughts.
- Effect of trim in ballast cases
- Wind resistance of model
- Treatment of wind resistance in prediction procedure

Some insights on this can be found in Wang, J. (2019)

As the question remains important both for performance prediction as well as for the evaluation of sea trials results, ITTC has decided to address this topic in a more focussed way by setting up a dedicated working group. The work will be based on the fundamental goal based standards that have been established by ITTC's Guideline on the determination of model-ship correlation factors (see also Section 16). The main goal of the newly established working group is providing benchmark relationships between speed power performance at different draughts. These can be used to check the validity of correlation approaches.

12. SHAFT G-MODULUS

12.1 Introduction

The G-Modulus of the propulsion shaft is one of the key uncertainties in assessing the speed power characteristics of ships by speed trials. The shaft power is derived from the shaft torsional deflection measured by strain gauges or optical sensor systems and multiplied by the G-modulus to obtain torque and thence power. This material property defines the ratio between the shear stress and the shear strain and can be expressed in the Young's E-modulus by means of the Poisson ratio ν viz.

$$G = E / (2(1 + \nu)) \quad (19)$$

In theory the G-modulus can be derived for the full shaft section. In reality, for the size and weight of today's propulsion shafts such tests are not practical and reliable. Also, the testing of shaft samples in tensile or torsion configurations has demonstrated large uncertainties.

For this reason, a default value of 82,400 MPa is used in ISO 15016:2015 and in the ITTC 2017 Procedure.

In this section both results from the recent work of ITTC PSS (2017) as well as from earlier research is reviewed.

12.2 Previous Work

Prior to 1970 several organizations proposed various values for the G-Modulus:

ITTC: 81,400 MPa based on the value presented by Mr. Sakuichi Togino (1936), based on tests of 36 shafts with a diameter in the range of 260-455 mm.

SNAME: 82,000 MPa based on the value found by Mr. John H. Brandan (1962) from specimen tests with Molybdenum-Vanadium steel at 27 degr. Celsius.

BSRA: 81,900 MPa based on measurements of 68 shafts by means of ultrasonic equipment.

In 1969-1971 the Japanese organization JSTRA (Japanese government MOT & Japanese Shipyards) conducted an extensive test campaign with 76 intermediate shafts. The shafts were conventionally twisted by weights on a torsion arm. This resulted in an average G-modulus of 82,200 MPa

The same group of Shipyards also measured 43 shafts by using ultrasonic equipment manufactured by Electronic Consultant Company that was also involved in the BSRA campaign. It was concluded that the ultrasonic measurement is more accurate than the conventional twisting method. Finally, the Shipyard group recommended 82,000 MPa.

In 2015 ISO and ITTC agreed to use a default value for the G-modulus equal to 82,400 MPa. This figure harmonized the values from ITTC 2014 and from ISO15016:2001 and corresponds to the value proposed by Fincantieri Shipyard in that same meeting in London.

12.3 Recent Research

Inspired by ISO and ITTC, Hyundai Heavy Industries (Lee, Tae-II (2016)) conducted extensive material tests on propulsion shafts to

establish the G-Modulus for use in speed power trials analysis. This work was executed in compliance with Class rules and regulations and supervised by DNV-GL in 2015-2016.

As the mechanical twisting of actual propulsion shafts for today’s merchant ships was considered practically impossible due to the size and mass of the intermediate shaft sections, the shear modulus was derived from tensile tests of material specimens taken from actual shafts. Three shafts were used; a 650 mm diameter intermediate shaft for a 162,000 m3 LNGC and two 480 mm diameter shafts for a 174,000 m3 LNGC.

In consultation with Class, the specimens were taken at several locations and orientations of the shaft cross sections at both ends of the shafts.

The test specimens were produced in compliance with ASTM E111-04 and DNV Ship Rule Pt.2, Ch.1, Sec.1. The tensile testing machines and technicians complied with KOLAS.

From the measured stress-strain curves the linear part between 40 and 65% of yield stress were used to derive the Young’s E-modulus. For the derivation of the shear G-modulus a Poisson ratio of 0.29 was taken from ASME Sec. II, Part D (2013).

The average results over multiple specimens per shaft as presented by Dr. Tae-II Lee to ITTC-PSS Committee in their meeting on June 15, 2016, are presented in Table 7.

Table 7

| Shaft # | No of test specimen | Average G-modulus [Mpa] | Standard Deviation [Mpa] |
|---------|---------------------|-------------------------|--------------------------|
| 1 | 6 | 85,691 | 9,858 |
| 2 | 8 | 83,123 | 4,190 |
| 3 | 8 | 89,571 | 18,381 |

It was stated by HHI that torsion tests on actual size propulsion ships is often impossible. HHI concluded that derivation of G-modulus

from tensile tests of shaft specimen results in unacceptably large variation.

12.4 Conclusions

Based on the above results, SOS concluded that the default value of the G-modulus to be used for speed power trials remains 82,400 MPa.

As stated in the Procedure, measured values of the actual propulsion shaft may be accepted provided that an adequate measurement procedure and certified equipment is used by qualified test engineers.

13. WATER TEMPERATURE AND DENSITY CORRECTION

13.1 General

The water temperature and density correction should be carried out in the same manner as ISO 15016. Sea water temperature and density may be measured by taking water samples at the trial site and from an inlet which is located at the same level as the ship's bottom. It is difficult to determine where the sample should be obtained, as discussed in the final report of the 28th ITTC.

The degree of the effect may be evaluated by some cases of sea trial and the environmental condition of the sea. For example, in some of the sea trial areas of China, water temperature normally changes within 3°C in different season (Table8).

From the sea trial records of VLOC series vessel (Table9), water temperature has about 20 °C change.

Table 8 Water Temperature changing with different season and depth

| | | East China sea | | Yellow sea | |
|-----------------------|--------|---|--------------------------|---|--------------------------|
| | | Temperature changing amplitude every day (°C) | Average Temperature (°C) | Temperature changing amplitude every day (°C) | Average Temperature (°C) |
| Surface layer | Winter | 0.6 | 9~12 | 0.5 | 2~10 |
| | Spring | 1.3 | 17~23 | 0.8 | 13~17 |
| | Summer | 0.9 | 26~29 | 2.1 | 24~27 |
| | Autumn | 0.5 | 17~26 | 2.0 | 13~14 |
| Middle layer (5m~10m) | Winter | 0.4 | 9~11 | 0.4 | 2~10 |
| | Spring | 1.4 | 16~23 | 0.4 | 12~15 |
| | Summer | 0.2 | 20~22 | 2.4 | 18~20 |
| | Autumn | 0.2 | 15~23 | 2.4 | 13~14 |

Table 9 Water Temperature conditions for the trials of VLOC series vessel at Ballast Condition

| Ship No. | Sea Trial Area | Water Temperature (°C) |
|----------|----------------|------------------------|
| 1# | Yellow sea | 5.5 |
| 2# | East China sea | 15.0 |
| 3# | East China sea | 14.0 |
| 4# | East China sea | 17.5 |
| 5# | Yellow sea | 19.5 |
| 6# | Yellow sea | 24.4 |
| 7# | Yellow sea | 25.0 |

According to the correction formula of ISO 15016, the power correctional values of different water temperature for 39000 DWT and 60000 DWT B.C were calculated and compared with the test results of power (Figure 46). When the temperature is higher than the reference value (15 °C), the speed correction is about -0.02kn interval per 2.5°C. If the temperature is lower than the reference value, the speed correction is about +0.02kn interval per 2.5°C.

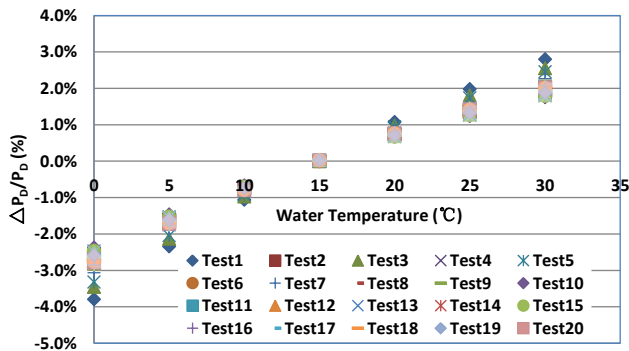


Figure 46 Correction of power for different water temperature (39000DWT B.C & 60000DWT B.C)

13.2 Conclusions

The Committee considered that the present correction method for the water temperature and density correction should be retained.

14. NOISE IN THE MEASURED DATA AND MEASUREMENT ERROR

14.1 General

The uncertainty of the speed and power performance is determined by the accuracy level of the measured values of shaft power and environmental disturbances. To reduce the uncertainty of the speed and power performance analysis during speed trial, it is recommended to use a reliable measurement system and to perform it in an ideal environmental condition such as still water, but it is not easy to conduct speed trials under ideal environmental conditions. Therefore, all results of speed and power performance include both the uncertainty of the measuring system and the uncertainty of added resistance from environmental conditions. The uncertainty analysis of speed / power performance was carried out based on raw data in sea trials. The speed power performance was estimated through the guideline of ISO15016, and Monte Carlo simulation was used for the analysis of uncertainties.

The results of the uncertainty analysis of the ship speed power performance during a double

run test at the MCR 75% condition showed expanded uncertainty due to the added resistance by wind (R_{AA}) which was $\pm 2\%$ and $\pm 12\%$ at each run. The uncertainty of added resistance due to waves (R_{AW}) was $\pm 16\%$, respectively (at a 95% confidence interval, $k=2$).

Table 10 Uncertainty of Resistance increase due to wind and waves

| Engine Load | Wind | | Waves | |
|-------------|-------|------------------|-------|------------------|
| | RAA | U (%) (95%, K=2) | RAW | U (%) (95%, K=2) |
| 50% 1st Run | -66.5 | ± 6 | - | - |
| 50% 2nd Run | 110.1 | ± 15 | 56.9 | ± 1.2 |
| 75% 1st Run | -89.8 | ± 2 | - | - |
| 75% 2nd Run | 152.6 | ± 12 | 81.3 | ± 1.2 |
| 90% 1st Run | -48.2 | ± 14 | - | - |
| 90% 2nd Run | 32.1 | ± 39 | 83.3 | ± 1.2 |

The expanded uncertainty of the measured delivered power (P_{Did}) converted to the ideal conditions was about $\pm 1.2\%$ as shown in Table 11. The uncertainty of the delivered power can be converted to an uncertainty of ship speed of about ± 0.1 knots.

Table 11 Uncertainty for corrected ideal power

| Engine Load | U (95%, K=2) (kW) | U (95%, K=2) (%) |
|-------------|-------------------|------------------|
| 50% of MCR | ± 164 | ± 1.2 |
| 75% of MCR | ± 227 | ± 1.2 |
| 90% of MCR | ± 265 | ± 1.2 |

The dominant component among the uncertainty factors for the delivered power in ideal conditions is the shaft power measurement system which accounts for about 60% of the total uncertainty. Hence, it is necessary to measure the shaft torque more precisely to reduce the uncertainty of the shaft power in sea trials.

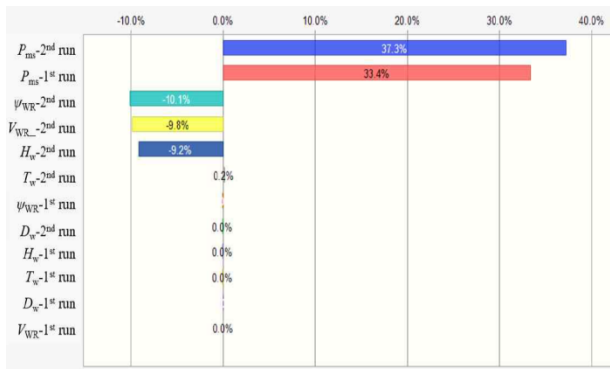


Figure 47 Sensitivity of corrected shaft power on basic input parameters (MCR 75%)

14.2 Conclusions

It is found that the expanded uncertainty of ideal power performance is about $\pm 1.4\%$ at the 95% confidence level ($k=2$). The influence of the uncertainty in the added resistance was minor due to moderate weather conditions, and thus the shaft power measurement system (standard uncertainty of the shear module) was the dominant effect.

15. UPDATE THE SPEED/POWER SEA TRIAL PROCEDURES 7.5-04-01-01.1

Main updates of the procedure during this term are as follows.

Shallow water correction. The committee accepted the Raven method exclusively concerning shallow water corrections and new water depth limitations for the applicability of shallow water corrections were established. Additionally, the appropriate formulae correcting vessel's speed achieved during speed trials were replaced by corrections of delivered power. The shallow water speed corrections based on the Lackenby method are excluded from the procedure.

Wave correction. A new wave-added resistance prediction method-SNNM was developed and validated extensively to adapt the situation when wave angle is larger than 45° from

heading and shipline is not available. After open validation in SOS and full discussion, SOS agreed to include SNNM into the sea trial procedure.

Wind averaging method. Limitations of wind averaging method were detected. The reasons for averaging method and exceptional case for averaged single run were presented (refer to 6.2).

Guidance on the location of anemometer was recommended (refer to part5)

Additional runs for sister vessels due to current change were updated. If after evaluation the vessel speed deviates more than 0.3 knots compared to the first ship of the series and "Mean of Means" method is used, the full run program as specified for the first ship shall be followed.

Finally, there was an update of the wind force coefficient database applied in the relevant appendix.

16. UPDATES TO THE GUIDELINE ON THE DETERMINATION OF MODEL-SHIP CORRELATION FACTORS

The guideline 7.5-04-05-01 had been first introduced by the 28th ITTC, so the last term has seen the first revision-period for this new guideline. Generally, the guideline addresses the standards and procedures according to which institutes shall derive their individual correlation schemes. The guideline in this sense defines minimum requirements and general guidance for this task. The major changes that have been incorporated into the new revision of the guideline are as follows.

The procedures and standards provided in the guideline are explicitly no longer limited to physical model testing. The general rules and requirements set out in the guideline may also be used for correlation in the context of CFD-calculations. Consequently, the wording was changed to "prediction" in general.

More detailed description of iterative approach for determination of a resistance-based correlation factor (i.e. C_A).

The description of the background and general approach has been extended giving a clearer explanation of the purpose of the guideline.

Furthermore, an example implementation of the procedure in Excel format was provided to the committee members for testing

16.1 Practical Procedure to Derive a Resistance-Base Correlation Factor (C_A)

The determination of C_A requires an iterative process as shown in Figure 48. This is necessary as the propulsive efficiency η_D represents a non-linear relationship between effective power P_E and delivered power P_D . For the determination of the correlation factor C_A , the values for η_H and η_R are taken from the model tests while the propeller efficiency η_0 is obtained from the propeller open water characteristics.

16.2 Required Size of Samples for a Reliable Determination of Correlation Factors

Each towing tank is using its own, specific regression model for the correlation scheme. The correlation formulae depend on a number of m variables.

The regression model may be derived by multivariate regression analysis. The significance of the individual parameters has to be tested by statistical instruments. In order to obtain statistical significant results, the sample has to be of a certain minimum size. This depends on the number of parameters used for the correlation scheme. According to Green (1991) the following rule of thumb may be used for the determination of required sample sizes:

$$n > 50 + 8 \cdot m \quad (20)$$

n number of samples, m number of independent variables in the regression formula.

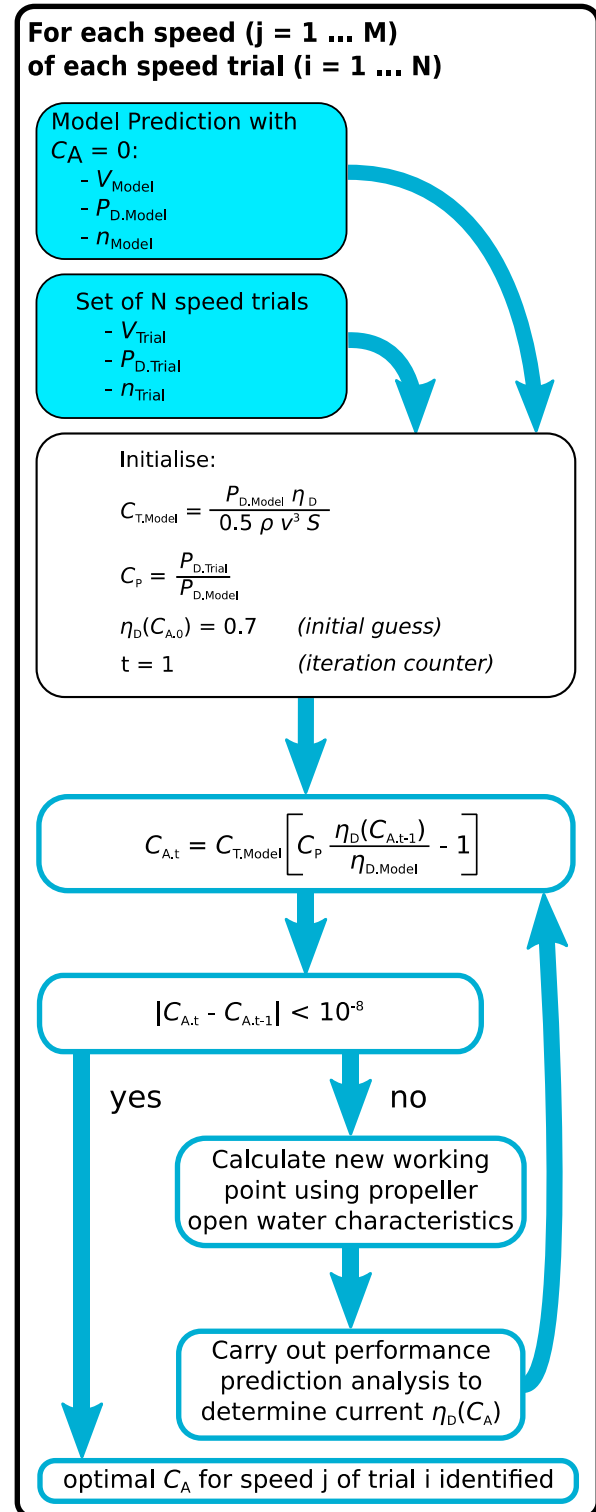


Figure 48. Determining optimal C_A iteratively

17. KEY PERFORMANCE INDICATORS FOR SHIPS IN SERVICE

There are multiple reasons for monitoring ship powering performance in service. A primary reason is to track increases in hull and propeller fouling, such that efficient performance of the vessel is ensured through appropriate timing of maintenance interventions, whether hull and/or propeller cleanings, or application of new coatings.

Other reasons may include weather routing for improved fuel efficiency, real-time ‘optimisation’ of draught and trim, feedback to designers for estimation of sea margin and feedback to towing tank organisations for correlation and research purposes. Recently, attempts to reduce fuel consumption by operators for environmental reasons as well as economic have placed greater emphasis on vessel fuel efficiency and hence performance monitoring.

The IMO mandating assignment of an Energy Efficiency Design Index (EEDI) and adoption of a Ship Energy Efficiency Management Plan (SEEMP) have placed greater regulatory focus on this area, in particular in requiring the verification of speed and power for the EEDI through accurate sea trials results.

Ongoing discussions at IMO on ‘short term measures’ to reduce Greenhouse Gas (GHG) Emissions from shipping are likely to increase the focus on operational measures to reduce fuel consumption. These discussions may result in a form of Carbon Intensity Index (CII) that will require determination of a ship’s powering performance in service as well as when newly built, for regulation. This will further increase emphasis on trustworthy measures of in-service power and speed and methods to compare fairly between loading, and encountered environmental, conditions. These measures – as with EEDI – are likely to require ongoing % reductions relative to a baseline performance. These baseline performances are derived through statistical analysis of fleet data pertaining at a particular time.

These baselines are distinct from those adopted by ship operators in managing hull and propeller fouling and associated maintenance interventions. In this latter case a baseline is usually established by monitoring powering performance when the ship is newly out of dry-dock and comparing subsequent performance to this baseline. The emphasis is therefore often on relative, rather than absolute, determination of performance. The challenge with modern coatings is in detecting relatively small changes in performance over a number of years, given the inherent scatter in measured data points arising from variations in vessel loading condition, ship speed, weather, sea currents, water temperature and salinity, engine performance and operational practices.

Traditionally, so-called ‘noon reports’ were the primary source of in-service data – consisting of a manual report of ship’s position, fuel consumed in 24hr period and an estimate of the prevailing wind and wave conditions made by an experienced mariner. In recent years these data are increasingly being supplanted by automatically recorded data at much smaller time intervals – often referred to as ‘high frequency’ or ‘continuous monitoring’ data. Examples of typical systems are given in section 19. Aldous et al (2015) compare uncertainties from these approaches and demonstrate that a continuous monitoring approach has much lower uncertainty than using noon reports, such that similar levels of uncertainty in power are determined from continuous monitoring data after 90 days at sea as from noon report data after 270 days at sea. It is considered that noon report data has too much uncertainty to be of great value to the ITTC community, although with automated collection of parameters it retains some value for long term monitoring of ship performance.

One problem with all measurements and analysis is the characterisation of the encountered wind and wave environment. Noon reports are often reliant on manual observation. Continuous monitoring systems typically record the anemometer as the means to determine wind

speed and direction. The measured relative wind requires correction to true wind, but this is a measurement of a disturbed wind field. Wave height is generally not recorded, but may sometimes be available from a MetOcean hindcast model. Potential uses of these data are discussed in Boom and Hasselaar (2014) and Lakshminarayanan and Hudson (2018). Recent developments in shipboard measurement of wave height are discussed in section 18.

Standards derived for analysis of ship performance data (ISO19030) therefore recommend a continuous monitoring approach. Most such analyses rely on monitoring performance through the derivation of speed power curves, or using Key Performance Indicators (KPIs) over time. Typically, these approaches focus on filtering and ‘binning’ data to derive a calm water condition. This reduces the influence of weather by filtering out data points for wind speed and wave heights above a threshold value and by retaining narrow ranges of draught and trim conditions (see, for example, Dinham-Peren and Dand, 2010). Such methods filter out a large amount of data, typically retaining only about 9-11% of the total dataset.

A major problem with such methods is the transparent and consistent definition of threshold values for data filtering (i.e. “less than x m wave height represents ‘calm water’”). These choices greatly affect derived speed power curves due to changes in the size of the resulting dataset. For this reason, the derivation of speed power curves should be avoided if possible unless accompanied by clear presentation of applied threshold values and justification for their selection.

An alternative approach is to correct or normalise the data by applying shaft power corrections for the effects of wind and waves. Boom and Hasselaar (2014) discuss the improvements that applying methods derived initially for sea trials correction can make to in-service performance assessment. Further recent developments in this approach are reviewed in section 21.

If sufficient data are available for analysis then a pure data-driven approach using machine learning techniques has been shown capable of predicting power with a mean error of 2% compared to measured power across the full range of ship loading condition, operational speed and encountered wind and waves for an LNGC carrier (Parkes et al, 2018).

Developments in data collection and processing techniques are covered well in the ‘Hull Performance and Insight Conference (HullPIC)’ series, annually since 2016.

For the monitoring of hull and propeller fouling it is common to use ‘speed loss’ as a performance indicator or KPI, as recommended in ISO19030 and aligned with some onboard systems and coating manufacturers. An alternative is to use ‘power (or resistance) increase’. Given the approximately cubic relationship between power and speed, the latter is more sensitive to small variations. With these performance indicators it is not possible to separate effects of hull fouling from propeller fouling, which can result in sub-optimal decisions around maintenance interventions. A complete separation of hull and propeller fouling is not possible without separate thrust and torque measurement on the propeller shaft. The small deflection of the propeller shaft due to thrust makes this extremely difficult, recent progress is discussed in section 20. Partial separation of propeller and hull effects is possible through careful consideration of the torque, propeller revolutions and ship speed.

Analysis of continuous monitoring data is key to realising operational efficiencies (draught, trim optimisation, weather routing, coating and maintenance strategies) and is likely to be central to international efforts to reduce Greenhouse Gas emissions from shipping. Presently there are few standards for the automated collection and analysis of such data. ISO19030 offers one standard, but is focused on filtering data, such that the dataset size is greatly reduced. There is potential in methods that correct, or normalise, data (as discussed in section 21) to increase

useful data and accuracy. Such methods offer the potential to provide insights into ship performance when combined with data from towing tank tests and CFD. Uncertainties remain regarding encountered wind and wave conditions and further investigation is recommended in these areas.

18. MORE ACCURATE MEASUREMENT OF ENVIRONMENTAL DATA

For the reliable evaluation of Ship's speed/power performance from in service performance monitoring, accurate measurement of encountered environmental conditions is of primary importance. Among the environmental data, encountered waves are the most difficult to obtain from onboard ships in service. For the routine recording of wave conditions in onboard log books, visually observed wave data have been used and is still normal practice today.

In recent years with the advancement of wave radar analysing technologies which evaluate wave directional power spectrum by analysing the scattering of the X-band radar signal caused by Bragg backscattering from the sea surface ripples (so-called "sea clutter") (e.g. Plant and Keller (1990), Lee et al. (1995), Nomiya and Hirayama (2003), Giron-Sierra and Jimenez (2010)), so-called "wave radar" systems provide by several manufactures (e.g. Miros WAVEX system, Ocean Waves WaMos II system) have increasingly employed as a wave measuring device in on-board performance monitoring. Some examples of wave measurements on ships in service are presented in the following and their effectiveness for ship performance monitoring is discussed.

Yoshida et al. (2015) presented results of wave-radar measurements on an iron ore carrier and comparison with the forecast and on-board visually observed data, see Figure 49. It is found that the agreement among the data is reasonably good but the wave-radar data tend to underestimate relative to other data, in particular in rough

wave conditions (wave height greater than 4m). In addition, they validated the wave radar data by comparing short-term estimations of pitch and roll motion calculated using the wave-radar data with measured ship motions. It is shown that estimations from radar wave data agree well with measured motion data except for higher wave cases.

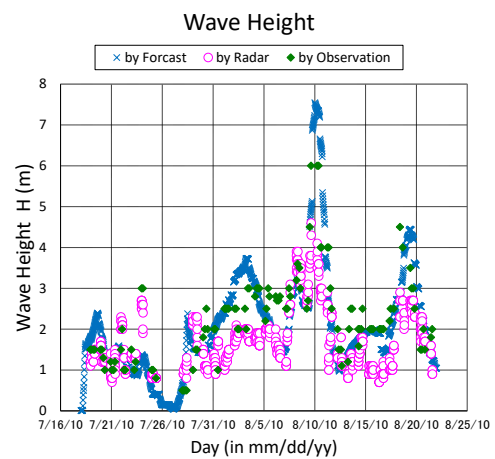


Figure 49 Comparison of wave-radar measured data with forecast and visually observed data. (Yoshida et al. 2015)

Lu et al. (2017) presented results of wave-radar measurements on a 28k DWT bulk carrier and comparison with the hindcast data calculated with NOAA's 3rd generation WW3 model (Stopa et al. (2016)). In their study, the hindcast wave data are firstly validated by comparing the short-term frequency spectra of ship's pitch motion in a similar way as Yoshida et al (2015) which is calculated using them, then comparison is made with the frequency spectra calculated from measured pitch data. Their comparison show good agreement between the short-term results with the measured data. Then they compared time-historical variations of wave statistical parameters (height, period, direction). They found that radar measured wave height and spectra lack reliability when significant wave heights exceed 4m, see Figure 50(WRF-Weather Research and Forecasting model, NCEP-National Center for Environmental Prediction model, ERA-European center for medium-range weather forecasts Re-Analysis

model). As for the reliability, they considered that the deficiency of the wave radar can be attributed to the large amplitude ship motions under which conditions the microwave radiation cannot accurately detect the sea surface ahead of the ship.

One of the drawbacks of the wave radar measurements is in that it cannot evaluate quantitatively the wave height or magnitude of wave energy by itself. That is, the measured reflection intensity of radar wave signal is not directly relating to the wave heights but roughness of the sea surface (ripples). Thus, the wave height is in most cases indirectly determined from the signal to noise (S/N) ratio of the radar in conjunction with calibration of the S/N ratio with wave height obtained from other devices or data sources. (e.g. Giron-Sierra and Jimenez (2010))

To deal with this drawback and reduce uncertainty arising from the use of S/N ratio, Iseki et al (2013) developed the hybrid Bayesian wave estimation method in which wave-radar data is incorporated into the ordinary Bayesian wave estimation method which estimate wave environment based on the wave buoy analogy with input of ship motion responses. It is shown that by using wave-radar data estimated directional wave energy spectrum can be improved and results in higher accuracy of wave period and direction. In this hybrid method, wave height, that is the magnitude of wave energy spectrum, is evaluated principally from the ship motions in a physically consistent manner without the need for empirical calibration. In their study, wave measurements were conducted on a 6,500 TEU class container ship on the north pacific route in winter of 2010.

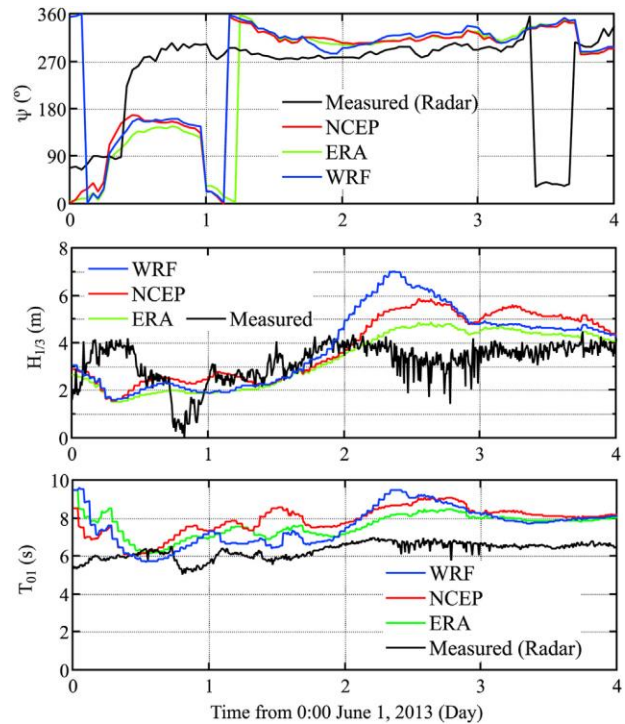


Figure 50 Comparison of observed and simulated (hindcast) wave directions, significant wave heights and periods. (Lu et al. 2017)

The wave statistical parameters estimated by the wave radar system using the proposed hybrid Bayesian system are compared with NOAA buoy data which is evaluated by referencing data from the nearest three NOAA wave buoys. Figure 51 shows the comparison of the estimated data (Bayes) and the buoy data. While the Bayes data well reproduce the time-historical variation, differences are relatively large in the order of 1 to 2m.

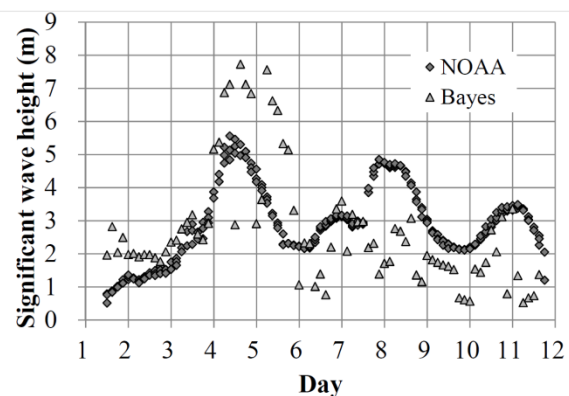


Figure 51 Comparison of estimated and measured wave heights. (Iseki et al. 2013)

As described in the above, the effectiveness of wave radar system as an onboard wave measuring device has not been thoroughly verified so far. Most of the verifications are made by the comparison with forecast or hindcast data. In addition, the agreement between the wave-radar data and forecast/hindcast data is not satisfactory. Comparison with the measured data from a wave buoy deployed close to the ship course is indispensable to conduct more detailed validations, in particular for the assessment of wave height estimation.

19. SPEED POWER PERFORMANCE RELATED MONITORING

Ship’s speed/power performance evaluation in service conditions has been of greater importance in recent years due to several reasons, including the introduction of EEOI (Energy Efficiency Operational Indicator). To achieve this on practical basis, reliable on-board monitoring of performance related parameters should be realized within reasonable costs justified from operational and financial point of view.

Contrary to the situations in builder’s speed/power sea trials conducted before delivery, performance monitoring on in-service ships need to be made automatically or by unskilled crews without assistance of experienced specialists normally attending the builder’s sea trials. Thus simplification of the monitoring procedures and robustness of the monitoring equipment are indispensable. To achieve this, most of the recent performance monitoring on in-service ships have employed system configurations connected to normal rule-mandate on-board operational data recording equipment including Voyage Data Recorder (VDR) and engine-room Monitoring System (EMS). (see Kim 2018, Orihara et al. 2019) Normally, most of the performance-related parameters are obtained from VDR and EMS except for encountered waves, ship motions and propeller/shaft thrust and torque for which special measuring devices is needed. Use of the equipment obviates the need

for the installation of special sensors and dedicated cabling for the performance monitoring. One example of these on-board monitoring systems is shown in Figure 52.

This monitoring system consists of a suite of sensors and a system’s PC to acquire, analyse and display data. Most of hull-related data (ship’s speed, course, heading wind, rudder angle etc.) are obtained from VDR as a LAN output data. Machinery-related data (fuel-oil flow rate, fuel-oil temperature, shaft power etc.) are obtained from engine-room data-logger (equivalent of EMS). Ship motions and encountered waves are optional monitoring items and measured by using dedicated motions sensors and a radar wave analyser.

Measured data are merged as a time-history data file of 20-min length containing all the monitored items. Then, statistical analysis of the time histories are conducted on the system’s on-board PC. Average, minimum, maximum, standard deviation, significant value and zero-up-cross period are calculated for all the data items. Statistically analysed data are automatically transmitted to the on-shore data server via satellite communication. Examples of performance analysis using the analysed data will be given in 5.5.

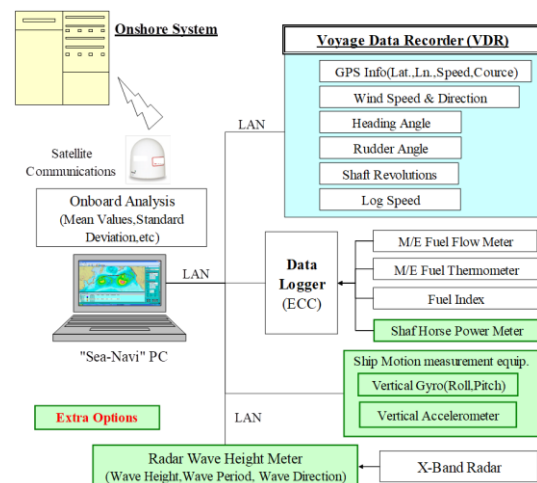


Figure 52 Configuration of “Sea-Navi” on-board monitoring system. (Orihara et al. 2019)

A set of on-board monitored parameters mentioned are basically common with those measured in the builder’s speed/power sea trials except for the speed through water (STW). Measurement of STW is normally made by a speed log (Doppler or Electro-magnetic type) and routinely in ship’s operation. However, it is well known that the accuracy of a speed log is quite sensitive to environmental disturbances and is prone to bias significantly.

To improve the accuracy of STW measurement, Sudo et al. (2018) developed Multi-Layered Doppler Sonar (MLDS) and evaluated its effectiveness through on-board measurements. Principles of MLDS are as follows. It transmits wideband ultrasonic waves which have multiple spectral peaks (= N). By doing so, about N times amount of data can be obtained by measuring Doppler shifts of each spectral peak at the same time independently. MLDS has been developed by using this function, which is continuously measuring the relative flow velocity at multi-layer of water as shown in Figure 53.

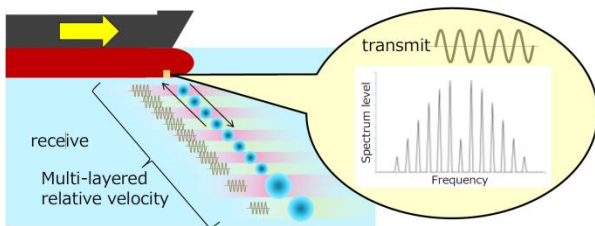


Figure 53 Multi-layered Doppler sonar. (Sudo et al. 2018)

Sudo et al. (2018) presented results of STW measurement using MLDS on a PCC and a tanker. Since draft/trim conditions affect flow field around a hull and measured STWs, measurements were made for a variety of draft/trim conditions. From the measured data depth-wise distribution of STW is established and the physically consistent STW value without effects of viscous and potential wake of the hull is obtained as a quasi-constant value at a depth sufficiently away from the hull. Figure 54 show an example of normalized depth-wise STW distribution for a specific draft/trim case. Although

MLDS can eliminate the effects of viscous and potential wakes, it cannot cope with the effect of depth-wise variation in tidal and ocean currents. Since the depth of STW measurement is 3 to 4 times a draft of ships, measured STWs may differ from those at depths from water surface to the bottom of a ship for the case of deep draft ships.

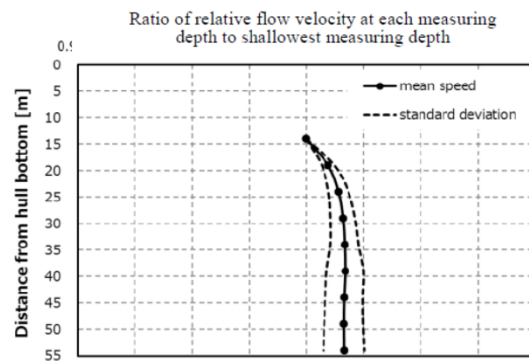


Figure 54 Overall average of relative flow velocity ratio at every layer to the shallowest layer. (Sudo et al. 2018)

MLDS were also applied to the near field flow measurements. Inukai et al. (2018) applied the MLDS for the full scale stern wake fields on a large container ship. Flows close to an operating propeller are measured and CFD simulation results.

On board monitoring thrust and torque. Observing the performance of the propeller and ship hull retrofits, it is important to measure the propeller performance from the hull resistance separately. For this, it is needed to measure propeller power, also the propeller thrust.

Application of an optical Propeller Thrust and Torque sensor, is a useful method to avoid unpredicted degradation of hull coating or propeller performance and able to separate the hull and propeller performance. In case the underwater area of the vessel's hull or the propeller is fouled or damaged, the monitoring system will indicate the cause and negative effects immediately. This is particularly useful when the propeller and bulbous bow are modified at the same time.

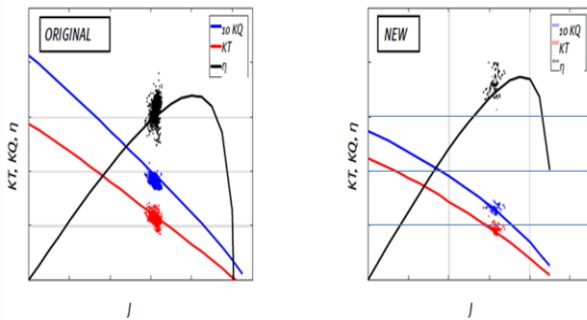


Figure 55 Monitoring the performance of different propeller

20. POSSIBILITIES TO ANALYSE SHIP PERFORMANCE ON A SINGLE RUN

Ship's speed/power performance evaluation in service conditions is normally conducted on a single run basis using speed through water (STW) as a reference speed. Since the on-board measured STWs frequently suffer from the bias and random errors, effective correcting procedures for these errors in STW are principal issues for achieving performance analysis on a single run. The other issue is the correction for the encountered disturbances to the standard or reference weather conditions. Since the weather conditions (wind & waves) and ship responses in service vary significantly depending on the operating requirements, monitored data should be corrected to unified reference conditions so that consistent evaluations can be made on the same basis.

For the correction of encountered disturbances, attempts employing the approach similar to ISO15016:2015 have been proposed, for instance, Kim et al. (2018), Orihara and Tsujimoto (2018). Among them, Kim et al. (2018) measured speed/power performance of the 300K bulk carrier in service. Measured data were analysed by their newly developed method based on ISO15016:2015 and compared with that of model test result under still water conditions without wind and wave effects. Figure 56 shows an example of speed/power monitoring results.

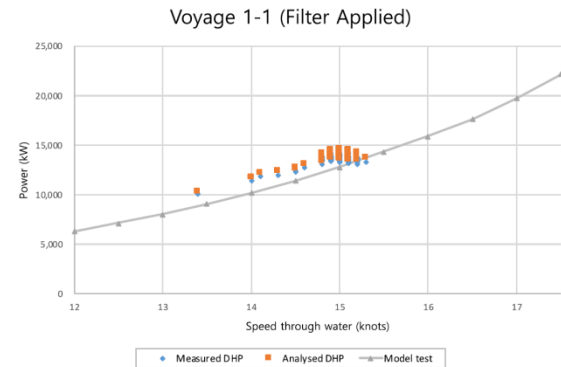


Figure 56 Analysis results of voyage 1-1 (after filtering). (Kim et al. 2018, 300K bulk carrier)

Orihara and Tsujimoto (2018) proposed full scale speed/power performance analysis method for the evaluation of performance under standard weather conditions according the Beaufort scale (BF) on a single run approach using STW as a reference ship speed. Corrections for wind and waves are similar to those in ISO15016:2015.

Orihara etc. (2019) presented speed/ power performance in service analysis results for a VLCC, a large bulk carrier and a PCTC using the method of Orihara and Tsujimoto (2018). In this study, analysed results were compared with estimated speed/power curves for conditions equivalent to BF=4, 5, 6. Examples of comparison are shown in Figure 57 and

Figure 58 for a VLCC and PCTC respectively. It is shown that analysed results agree reasonably well with the estimated curves for a range of weather conditions. In these comparisons bias error of STW measurement is corrected as a combination of fouling/aging effect by subtracting the power difference between analysed speed/power curve for BF=0 (no wind & wave effects) and estimated curve from still-water resistance/self-propulsion model test results.

Limelette et al (2018) presented results of a comparison between filtering and normalisation approaches to determine calm water performance, for an LNGC vessel from measured data over an 18 month period. Filtering criteria were

applied to determine calm water performance, namely that significant wave height (from MetOcean hindcast model) <1.5m, true wind speed <10 knots and the difference between the STW and SOG <1 knot. Correction, or normalisation, of the data using STAWAVE-1 and STAWAVE-2 was performed for comparison purposes, respecting the wave correction limits of these methods and neglecting correction for wind resistance. For this ship, which is considered as large and where encountered ship motions within the wave limit ranges was considered small, correction of data exhibited less scatter using STAWAVE-1 as compared to STAWAVE-2. Within the ship operating range of 9-19 knots, there was a maximum difference of 6% between results for calm water power derived by filtering and normalisation. This further suggests that correction may be a suitable alternative to filtering to obtain calm water power for vessels at sea from measured data.

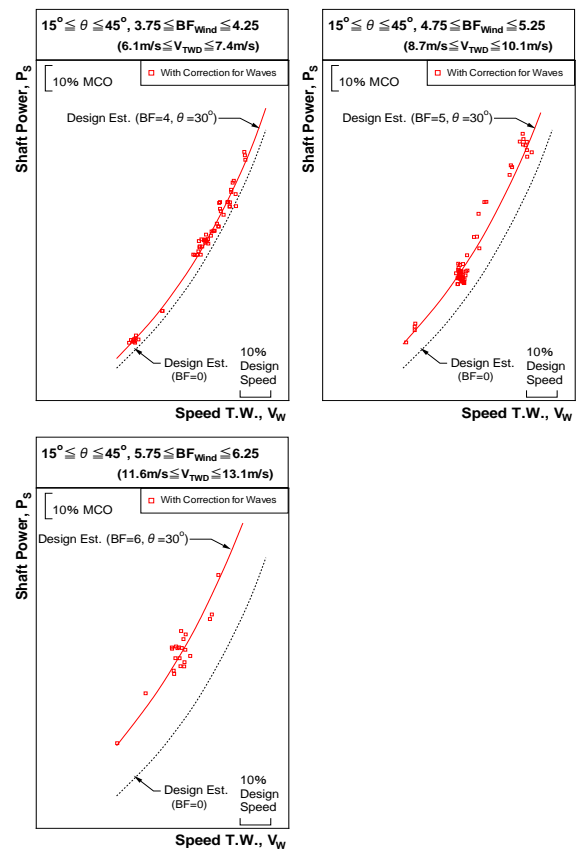


Figure 57 Measured and corrected speed/power performance for Ship A, $15\text{ deg.} \leq \theta \leq 45\text{ deg.}$ (Orihara et al. 2019, VLCC in bow sea conditions)

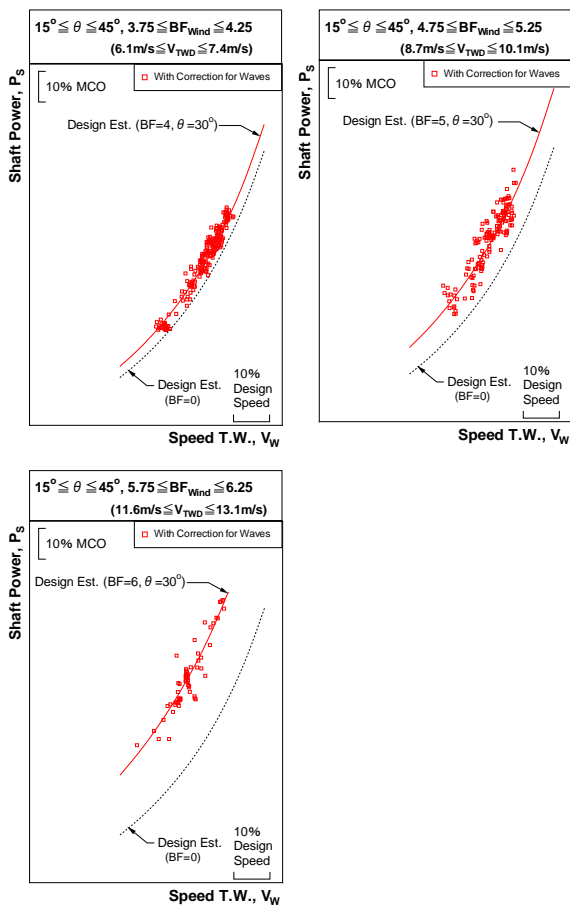


Figure 58 Measured and corrected speed/power performance for Ship C, $15^\circ \leq \theta \leq 45^\circ$. (Orihara et al. 2019, PCTC in bow sea conditions)

Speed/power performance monitoring and analysis methods described above can be readily conducted on in-service ships without small additional cost and considered as one of the viable approach to the analysis of the ship performance on a single run. In addition, they can cope with the ship's conditions not evaluated in the builder's trials such as fully loaded conditions for dry cargo ships or in rough weather conditions. So, their verification on a wide range of ships with an improvement of STW measurement is expected in the future.

21. EXPLORE 'SHIP IN SERVICE' ISSUES TO GET FEEDBACK TO TOWING TANKS

21.1 Applicability of Unmanned Vehicles and Devices

Airborne, underwater and floating devices are examples of unmanned vehicles that are effective in evaluating the performance of ships in service. Air drones are often used to monitor exhaust gas emissions, while underwater drones are used for water quality surveys and mapping the floors of the oceans. Although floating drones are used in the same way as underwater ones, and the drones have not obtained enough information that will be useful for providing feedback on actual operational performance, "Aquatic Drones (Aquatic Drones, 2018)" is introduced as an example of a floating drone that can be used to collect information that may be useful for estimating actual ship performance. Aquatic Drones are maritime robots that collect data autonomously. It is a multi-use platform with a wide range of sensors such as the radar for detection of ships, AIS system for ship tracking, camera and LIDAR for distance calculation and GPS for positioning. It can operate at sea in 10-18 hours on lithium batteries. If the seakeeping ability would be improved, it may be possible to measure wave height and directions or wind speed and directions or current information which are valuable for performance evaluation in actual seas.



Figure 59 An image of Aquatic Drones' surface platform.

22. MONITORING THE NEW INFORMATION AND COMMUNICATION TECHNOLOGIES APPLIED ON BOARD SHIPS

22.1 Overview

Although on board ICT of recent date is often used to confirm the integrity of the hull structure and main engine from land, the main purpose is to prevent accidents and respond quickly to breakdowns. Thanks to that, the communication environment between ship and land has improved dramatically. However, there are few introductions of the noticeable progress of the on-board monitoring instruments. LIDAR laser scanner technology is one of the few promising technologies.

22.2 Practical Example of LIDAR System

MARIN is conducting a demonstration test of wind velocity distribution measurement using LIDAR (Light Detection and Ranging) system in WINDLASS-JIP and aiming for practical use. Measurement campaign at exposed berth including 3-D wind field measurement by LIDAR wind scanner and mooring line loads by load cells will be implemented (WINDLASS-JIP, 2019). In addition, Pichugina measured the vertical wind velocity distribution using a LIDAR system installed on board a ship (Pichugina, 2012). The comparisons with more conventional measurement systems, such as rawinsondes, are shown and the effectiveness of LIDAR system are presented. However, such published and actual examples are limited, technologies for the prediction of ship performance need to be continually investigated.



Figure 60 Doppler LIDAR scanner on a vessel [Pichugina, 2012]

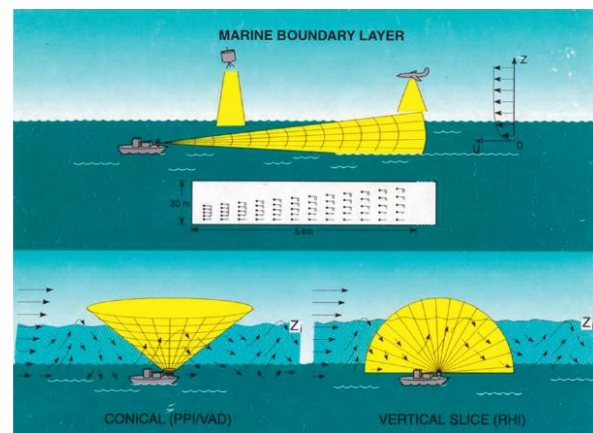


Figure 61 Common scanning patterns used by LIDAR system [Pichugina, 2012].

23. CONCLUSIONS AND RECOMMENDATIONS

23.1 Main Conclusions

- Raven (2016) method has been accepted exclusively as a shallow water correction method, and upper limit of shallow water has been cancelled to avoid discontinuity and low limit redefined on the basis of study. Lackenby method has been skipped.
- Detailed survey on the development of CFD methods for wave-added resistance shows that the deviation in comparison to results obtained from model tests is found to be in the range of 20%. In tendency short wave lengths are affected by higher errors. Most of the comparisons are made in head wave cases only. Assessment of the accuracy in waves other than head waves is scarce.
- A new full directional wave-added resistance method has been openly and

intensively validated by SOS committee. The proposed method is included in the final report of the committee and the sea trial procedure.

- d) Limitations of averaging wind correction method investigated and discussed extensively. Averaging method has considered the influence of superstructure. However, for large ships, when double run takes long time, the accuracy of averaged method decreases. To overcome this disadvantage, new testing instrumentation such as Lidar is proposed.
- e) Guidance on the location, and type of the anemometer suggested.
- f) A comparative study with CFD on wind resistance coefficient has been initiated and conducted. New approach for non-dimensionalising wind resistance coefficients has been proposed and implemented.
- g) A new guideline for the CFD-based Determination of Wind Resistance Coefficients has been established. It provides guidance for CFD based derivation of wind resistance coefficients.
- h) Number of double runs for sister ships has been clarified.
- i) The guideline for derivation of correlation factors has been reviewed and updated by the committee.
- j) The committee has reviewed the state of the art related to in-service performance monitoring including collection of data, analysis methods as well as filtering of data.
- k) The speed/power sea trial procedure 7.5-04-01-01 has been further updated to reflecting all research findings so far.
- l) For shallow water model testing towing tanks are normally too limited in width. Therefore, results need to be corrected for tank wall effects.

23.2 Recommendations to the Full Conference

- a) Adopt the revised Procedure 7.5-04-01-01: Preparation, Conduct and Analysis of Speed/Power Trials (2021)
- b) Adopt the revised Guideline 7.5-04-01-02: Guideline on the determination of model-ship correlation factors at different draughts (2021)
- c) Adopt the new Guideline on the CFD-based Determination of Wind Resistance Coefficients (2021)

23.3 Recommendations for future work

1. Address issues related to hull and propeller surface roughness such as:

- a) Definition of roughness properties
- b) Components of roughness
- c) Measurement of roughness
- d) Effects of roughness on in-service performance including filtering and analysis methods for evaluating hull and propeller performance separately
- e) Roughness usage in performance prediction and cross effects with correlation

2. Provide technical support to ISO and IMO in further development of approaches to in-service performance monitoring (e.g. ISO19030)

3. Address the following aspects of the analysis of speed/power sea trial results:

- a) Initiate and conduct speed trials on commercial ships on deep and shallow water to further validate Raven method.
- b) More validation on wave-added resistance methods, and recommend better method if appropriate.
- c) Investigate the influence of water depth on the hull-propeller interaction (thrust deduction, relative rotative efficiency)
- d) Continue reviewing state-of-the-art of added resistance assessment by means of CFD.

e) Explore and monitor new developments in instrumentation and measurement equipment relevant for sea trials and in-service performance assessment (e.g. wind, waves, thrust, speed through water).

4. Further investigate and validate draft dependency of model-ship correlation.

5. Study accuracy of CFD for shallow water applications.

6. Update the speed/power sea trial procedures 7.5-04-01-01.1 where appropriate.

7. Support ISO in updating ISO15016 in compliance with 7.5-04-01-01.1(2021).

8. Update guideline for determination of model-ship correlation factors.

9. Update guideline on CFD-based wind coefficient; in particular re-assess database of wind resistance coefficients and update it according to the new procedure for non-dimensionalising.

24. REFERENCES

Aldous, L., Smith, T., Bucknall, R., Thompson, P., 2015, "Uncertainty Analysis in Ship Performance Monitoring", Ocean Engineering, Vol. 110, pp. 29-38.

Aquatic Drones, 2018, <https://www.aquaticdrones.eu/>

Boom, H.J.J. v. d., Huisman, H. & Mennen, F., "New Guidelines for Speed/Power Trials", SWZ-Maritime, January and February 2013.

Boom, H.J.J. and Hasselaar, T.W.F., 2014, "Ship Speed power Performance Assessment", SNAME Maritime Convention, Houston, Texas, USA, 12pp.

Brandan, John H., 1962, D.T.M.S. Report No. 1517.

Dinham-Peren, T.A. and Dand, I.W., 2010, "The need for full scale measurements", RINA William Froude Conference: Advances in Theoretical and Applied Hydrodynamics – Past and Future, Portsmouth, UK.

D.W. Seo., M.S. Kim., S.Y. Kim, 2019. "Uncertainty Analysis for Speed and Power Performance in Sea Trial using Monte Carlo Simulation" in Korean, Journal of the Society of Naval Architects of Korea, Vol. 56, No. 3, pp. 242-250

Fujii, H. and Takahashi, T., 1975, "Experimental study on the resistance increase of a ship in regular oblique waves", Proceedings, 14th International Towing Tank Conference, Ottawa, CANADA, Vol. 4, pp 351-360.

Giron-Sierra, J. M. and Jimenez, J. F., 2010, "State-of-the-Art of Wave Measurement for Ship Motion Prediction", Proceedings, 8th IFAC Conference on Control Applications in Marine Systems, Rostock-Warnemunde, Germany.

Green, S. B., 1991, "How many subjects does it take to do a regression analysis?", Multivariate Behavioral Research, 26(3), 499–510. https://doi.org/10.1207/s15327906mbr2603_7

Grin R. "On The Prediction Of Wave Added Resistance With Empirical Methods", Journal of Ship Production and Design, Vol. 30, No. 4, November 2014, pp. 1–11

Grin R. and Boom H. Van den, 2020, "Correlation study SNNM - SPAWAVE -FATIMA", MARIN memo.

Guo, H., and Wan, D., 2019, "Study of Wave Added Resistance and Motions of KCS in Waves with Different Wave Lengths", Proceedings, 38th International Conference on Ocean, Offshore and Arctic Engineering, Glasgow, Scotland, UK.

- Hoffmann, P., 2017, "CFD Analysis, ship model HSBC", Technical Report No. RH-2017/T-008E, CTO S.A., Gdansk, Poland
- Hossain, M.A., Wu, P.-C., Shibano, Y. and Toda, Y., 2018, "Forces, Ship Motions and Velocity Wake Field for KRISO Container Ship Model in Regular Head Waves", Proceedings, 28th International Ocean and Polar Engineering Conference, Sapporo, JAPAN.
- International Maritime Organization, MEPC 70/INF.30. 2016. "Supplementary information on the draft revised Guidelines for determining minimum propulsion power to maintain the maneuverability of ships in adverse conditions", London, UK.
- International Standards Organisation (ISO), 2015, ISO 19030, "Ship and Marine Technology – Measurement of Changes in Hull and Propeller Performance".
- Inukai, Y., Sudo, Y., Osaki, H., Yanagida, T., Mushiake, M. and Kawanami, S., 2018, "Extensive Full scale Measurement on Propeller Performance of 14000 TEU Container Ship", Proceedings, 3rd Hull Performance & Insight Conference, Redworth, UK, pp 27-35.
- Iseki, T., Baba, M. and Hirayama, K., 2013, "Hybrid Bayesian wave Estimation for Actual Merchant Vessels", Proceedings, 10th International Conference on Marine Navigation and Safety of Sea Transportation, Gdynia, Poland.
- ITTC Procedures, "Preparation, Conduct and Analysis of Speed/Power Trials, Procedure", 7.5-04-01-01.1, 2017.
- Kaiser, M., 2016, "Results of aerodynamic model tests for HSBC", Technical Report No. RH-2016/T-104E, CTO S.A., Gdansk, Poland
- Kaiser, M., 2019, "Results of model tests in wind tunnel, ship model JBC", Technical Report no. RH-2019/T-078E, CTO S.A., Gdansk, Poland.
- Kim, H., Park, B.- J. and Van, S.- H., 2018, "Analysis for the Powering Performance of Dry Cargo Ship in Operation", Proceedings, 28th International Ocean and Polar Engineering Conference, Sapporo, JAPAN.
- Kim, M., Hizirb, O., Turana, O. and Incecika, A., 2017, "Numerical studies on added resistance and motions of KVLCC2 in head seas for various ship speeds", Ocean Engineering, Vol. 140, pp 466-476.
- Kim, M., Hizirb, O., Turana, O., Day, S. and Incecika, A., 2017, "Estimation of added resistance and ship speed loss in a seaway", Ocean Engineering, Vol. 141, pp 465-476.
- Kim, Y.-C., Kim, K.-S., Kim, J., Kim, Y., Park, I.-R. and Jang, Y.-H., 2017, " Analysis of added resistance and seakeeping responses in head sea conditions for low-speed full ships using URANS approach", International Journal of Naval Architects and Ocean engineers, Vol. 9, pp 641-654.
- Kume, K., Ohba, H., Orihara, H., Mizokami, S., "Wind Velocity Profile and Representative Wind Velocity for Wind Resistance Measurement of Ship Models", Journal of JASNAOE, Vol.30, pp.1-13, 2019.
- Kume, K., Bielicki, S., Kobayashi, H., Ohba, H., "Validation of dimensionless method using height average wind velocity for wind forces", Journal of JASNAOE, Vol.31, 2020.
- Lakshmyanarayana, P.A. and Hudson, D.A., 2018, "Is Wave Height Necessary to Determine Ship Performance in Calm Water from Measurements?", Proceedings of 3rd Hull Performance and Insight Conference: Hull-PIC '18, Redworth, UK, pp. 335-346.
- Lee, P. H. Y., Barter, J. D., Beach, K. L., Hindman, C. L., Lake, B. M., Rungaldier, H. and Yuen, H. C., 1995, "X Band Microwave

- Backscattering from Ocean Waves", Journal of Geophysical Research, Vol. 100(C2), No.16, pp 2591-2611.
- Lee, J.H., Seo, M.G., Park, D.M., Yang, K.K., Kim, K.H. and Kim, Y., 2013, "Study on the effects of hull form on added resistance", Proceedings, 12th International Symposium on Practical Design of Ships and Other Floating Structures, Changwon, KOREA, pp 329-337.
- Lee, Tae-Il, 2016, Presentation in 28th ITTC PSS Committee meeting on June 15.
- Limelette, M., Lakshmyraranana, P.A. and Hudson, D.A., 2018, "Derivation of the Calm Water Performance of a Ship Through Normalisation of Shaft Power from Full Scale Measurements", Proceedings of RINA International Conference on Full Scale Ship Performance, London, 7pp.
- Liu S., Papanikolaou A. and Zaraphonitis G. (2011), "Prediction of Added Resistance of Ships in Waves", Ocean Engineering, Vol. 38, pp.641–650.
- Liu S., Papanikolaou A. and Zaraphonitis G. (2015), "Practical approach to the added resistance of a ship in short waves", Proceedings of the 25th International Offshore and Polar Engineering Conference, KONA-USA, Vol. 3, pp. 11-18.
- Liu S. and Papanikolaou A. (2016a), "Fast approach to the estimation of the added resistance in head waves", Ocean Engineering, Volume: 112, pp. 211-225.
- Liu S. and Papanikolaou A., (2016b), "Prediction of the added resistance of ships in oblique seas", Proceedings of the 26th International Offshore and Polar Engineering Conference, Rhodes, Greece.
- Liu S., Shang B., Papanikolaou A. and Bolbot V. (2016), "Improved formula for estimating the added resistance of ships in engineering applications", Journal of Marine Science and Applications, Vol. 15(4), pp. 442-451.
- Liu S. and Papanikolaou A. (2019), "Approximation of the added resistance of ships with small draft or in ballast condition by empirical formula", Proceedings of the Institution of Mechanical Engineers, Part M: Journal of Engineering for the Maritime Environment, Vol. 233(1), pp. 27-40.
- Liu S., Papanikolaou A., Feng P., and Fan S. (2019), "A multi-level approach to the prediction of the added resistance and powering of ships in waves", Proceedings of the 38th International Conference on Ocean, Offshore and Arctic Engineering, Glasgow, Scotland.
- Liu S. and Papanikolaou A., (2020), "Regression analysis of experimental data for added resistance in waves of arbitrary heading and development of a semi-empirical formula", Ocean Engineering, <https://doi.org/10.1016/j.oceaneng.2020.107357> .
- Lu, L. F., Sasa, K., Sasaki, W., Terada, D., Kano, T. and Mizojiri, T., 2017, "Rough wave simulation and validation using onboard ship motion data in the Southern Hemisphere to enhance ship weather routing", Ocean Engineering, Vol. 144, pp 61-77.
- MARICAR (2016-2018). Seakeeping and added resistance in waves. Joint Industry Project of NTUA-Ship Design Laboratory and MARIC, Athens/Shanghai.
- MARIN, WINDLASS-JIP, 2019, <https://www.marin.nl/jips/windlass>
- MEPC 72/INF.15, Study on application of ISO 15016:2015 during the implementation of amendments to the Guidelines on survey and certification of the Energy Efficiency Design Index (EEDI), 2 February 2018.
- Moat, B.I., Yelland, M.J. and Molland, A.F., 2005a, "The effect of ship shape and

- anemometer location on wind speed measurements obtained from ships”, 4th International Conference on Marine Computational Fluid Dynamics, pp 133-139.
- Moat, B.I., Yelland, M.J., Pascal, R.W. and Molland, A.F., 2005b, “An Overview of the Airflow Distortion at Anemometer Sites on Ships”, International Journal of Climatology, Vol. 25., pp 997-1006.
- Moat, B.I., Yelland, M.J. and Molland, A.F., 2006a, “Quantifying the Airflow Distortion over Merchant Ships. Part I: Validation of a CFD Model”, Journal of Atmospheric and Oceanic Technology, Vol. 23, pp 341-350.
- Moat, B.I., Yelland, M.J. and Molland, A.F., 2006b, “Quantifying the Airflow Distortion over Merchant Ships. Part I: Application of the Model Results”, Journal of Atmospheric and Oceanic Technology, Vol. 23, pp 351-360.
- Nakamura, S., and Naito, S., 1977, "Propulsive Performance of a Container Ship in Waves", Naval Architecture & Ocean Engineering, Vol. 15, pp 24-48.
- Nomiyama, D. H. and Hirayama, T., 2003, "Evaluation of marine radar as an ocean-wave-field detector through full numerical simulation", Journal of Marine Science and Technology, Vol. 9, No.2, pp 88-98.
- Ohashi, K., Hino, T., Kobayashi, H., Onodera, N. and Sakamoto, N., 2019, "Development of a structured overset Navier–Stokes solver with a moving grid and full multigrid method", Journal of Marine Science and Technology, Vol. 24, No.3, pp 884-901.
- Orihara, H. and Yoshida, H., 2018, "A validation study of CFD simulations of a tanker in ballast condition advancing in waves ", Proceedings, 28th International Ocean and Polar Engineering Conference, Sapporo, JAPAN.
- Orihara, H. and Tsujimoto, M., 2018, "Performance Prediction of Full scale Ship and Analysis by means of On-board Monitoring. Part 2: Validation of Full scale Performance Predictions in Actual Seas", Journal of Marine Science and Technology, Vol. 23, No.4, pp 782-801.
- Orihara, H., Yoshida, H. and Takagishi, K., 2019, "Full scale Performance Monitoring of Large Merchant Ships and Comparison with Theoretical Predictions", Proceedings, 29th International Ocean and Polar Engineering Conference, Honolulu, Hawaii, USA.
- Papanikolaou A., and Nowacki Z. (1980), “Second-Order Theory of Oscillating Cylinders in a Regular Steep Wave”, Proc. 13th ONR Symp., Tokyo, pp. 303-333.
- Papanikolaou A. and Zaraphonitis G., (1987), “On an improved method for the evaluation of second-order motions and loads on 3D floating bodies in waves,” Journal Schiffstechnik, Vol. 34, pp.170-211.
- Papanikolaou, A., Bitner-Gregersen E., El Mochtar, O., GuedesSoares, C., Reddy, R., Spengler, F., Shigunov, V., Zaraphonitis, G., Energy Efficient Safe Ship Operation (SHOP-ERA) (2015), Proc. 12th Int. Marine Design Conference IMDC2015, University of Tokyo and Soc. Of Naval Arch. And Ocean Engineers of Japan, 11-14 May 2015, Tokyo, Vol. I, pp.132, ISBN 978-4-930966-04-9.
- Park, J., Jang, J., Kim, S. (2016). Full load speed trial of 8000TEU container vessel, Proceedings of the 13th International Symposium on Practical Design of Ships and Other Floating Structures (PRADS' 2016). Technical University of Denmark.
- Parkes, A.I., Sobey, A.J. and Hudson, D.A., 2018, “Physics-based shaft power prediction for large merchant ships using neural networks”, Ocean Engineering, Vol. 166, pp. 92-104.

- Pichugina, Y., "Doppler Lidar-Based Wind-Profile Measurement System for Offshore Wind-Energy and Other Maritime Boundary Layer Applications", Journal of Applied Meteorology and Climatology, pp.327-349, 2012.
- Plant, W. J. and Keller, W. C., 1990, "Evidence of Bragg Scattering in Microwave Doppler Spectra of Sea Return", Journal of Geophysical Research, Vol. 95(C9), pp 299-310.
- Raven, H.C., "A computational study of shallow water effects on ship viscous resistance.", 29th Symp. Naval-Hydrodynamics, Gothenburg, Sweden, 2012.
- Raven, H.C., "A new correction procedure for shallow water effects in ship speed trials", PRADS 2016, Copenhagen, Denmark, 2016.
- Raven, H.C., "Shallow water effects in ship model testing and at full scale", 5th MASHCON, Oostende, Belgium, 2019.
- Raven, H.C., "A method to correct shallow water model tests for tank wall effects." Jnl Marine Science Techn., Vol.24-2, June 2019.
- Sadat-Hosseini, H., Wu, P., Carrica, P., Kim, H., Toda, Y. and Stern, F., 2013, "CFD verification and validation of added resistance and motions of KVLCC2 with fixed and free surge in short and long head waves", Ocean Engineering, Vol. 59, pp 240-273.
- Sadat-Hosseini, H., Sanada, Y., Stocker, M., Stern, F., Toxopeus, S., Castiglione, T., Simonsen, C. and Otzen, J. F., 2015, " KCS Added Resistance for Variable Heading ", Proceedings, Workshop on CFD in Ship Hydrodynamics, Tokyo, JAPAN.
- Sadat-Hosseini, H., Toxopeus, S., Kim, D. H., Sanada, Y., Stocker, M., Simonsen, C., Otzen, J. F., Toda, Y. and Stern, F., 2015, "Experiments and Computations for KCS Added Resistance for Variable Heading", Proceedings, 5th World Maritime Technology Conference, Providence, Rhode Island, USA.
- SHOPERA (2013-2016). "Energy Efficient Safe Ship Operation", EU funded FP7 project, Grant Agreement number 605221, <http://www.shopera.org>, coordination by NTUA-Ship Design Laboratory.
- Simonsen, C., D., Otzen, J., F., Joncquez, S. and Stern, F., 2013, " EFD and CFD for KCS heaving and pitching irregular head waves ", Journal of Marine Science and Technology, Vol. 18, pp 435-459.
- S.M Oh., D.Y. Kang., S.H. Choi., D.Y. Lee., B.K. Kim, 2018. "Characteristics of wind speed and direction during sea trials of ships", Proceedings of the 28th International OCEAN and POLAR Engineering Conference, Vol. 4, pp. 879-886.
- Stopa, J. E., Arduin, F, Babanin, A. and Zieger, S., 2016, "Comparison and validation of physical wave parameter-izations in spectral wave models", Journal of Ocean Modelling, Vol. 103, pp 2-17.
- Strasser, C., 2018, "Wind tunnel tests, ship model HSBC", Technical Report No. 2789/01, SVA GmbH, Vienna, Austria.
- Strasser, G. et. al, 2014 "A Verification of the ITTC/ISO Speed/Power Trials Analysis", Journal of Marine Science and Technology.
- Sudo, Y., Igarashi, N., Yonezawa, T., Mushiake, M. and Kawanami, S. and Hino, T. 2018, "Improvement of Measuring Accuracy of Ship's Speed through Water by using MLDS (Multi-Layered Doppler Sonar)", Proceedings, 3rd Hull Performance & Insight Conference, Redworth, UK, pp 275-284.
- Togino, Sakuichi, 1936, title unknown, Japanese Society of Naval Architects and Ocean Engineers, No. 59.

- Tuck, E.O. and Taylor, P.J., 1970, "Shallow Water Problems in Ship Hydrodynamics", Proceedings 8th Symposium on Naval Hydrodynamics, Washington DC.
- Wang, J., Yu, H. & Feng, Y. Feasible study on full scale delivered power prediction using CFD/EFD combination method. J Hydrodynamics 31, 1250–1254 (2019). <https://doi.org/10.1007/s42241-019-0075-4>
- Yasukawa, H., 2019, "Speed Trial Analysis Method Eliminating the Need for External Disturbance Data", Ship Technology Research, Vol. 66, pp 135-149.
- Yasukawa H., Hirata N., Matsumoto A., Kuroiwa R., Mizokami S. (2019), "Evaluations of wave-induced steady forces and turning motion of a full hull ship in waves", Journal of Marine Science and Technology, Vol. 24(1), pp. 1-15.
- Yoshida, H., Orihara, H. and Yamasaki, K., 2015, "Long-term Wave Measurement by an Onboard Radar Wave Meter and Prediction of Ship Motions based on the Onboard Wave Measurement", Proceedings, 34th International Conference on Ocean, Offshore and Arctic Engineering, St. John's, Newfoundland, CANADA.
- Zaraphonitis, G., Papanikolaou, A., (1993) "Second-Order Theory and Calculation of Motion and Loads of Arbitrarily Shaped 3D Bodies in Waves", Marine Structures, Vol. 6, pp. 165-185.